

**A TALL TOWER WIND
INVESTIGATION OF NORTHWEST MISSOURI**

A Thesis
Presented to
The Faculty of the Graduate School
At the University of Missouri–Columbia

In Partial Fulfillment
Of the Requirements for the Degree
Master of Science

By
RACHEL REDBURN

Dr. Neil I. Fox, Thesis Supervisor

AUGUST 2007

The undersigned, appointed by the Dean of the Graduate School,
have examined the thesis entitled

A TALL TOWER WIND INVESTIGATION OF NORTHWEST MISSOURI

Presented by Rachel N. Redburn

A candidate for the degree of Master of Science

And hereby certify that, in their opinion, it is worthy of acceptance.

Dr. Neil I. Fox

Dr. Anthony R. Lupo

Dr. Christopher K. Wikle

Acknowledgements

I would like to first thank my advisor, Dr. Neil Fox, for his guidance in constructing and executing this research project. His direction and advice aided me to no end. Without his assistance the demands of this research project would have been impossible for me to complete.

I would also like to thank the other members of my thesis committee, Dr. Anthony Lupo and Dr. Chris Wikle, for their contributions and assistance. Their vast knowledge and helpful comments helped to better my thesis. Support from all these individuals motivated me to complete this project and develop a sincere interest in wind resource development.

I would also like to thank the entire Atmospheric Science faculty for providing me with the best education possible. I feel that our department has the most attentive professors and it is their sincere concern for education that makes this program wonderful and very much worthwhile. Thank you.

Lastly, I would like to thank the sponsors of this research project. Without their financial support this project may have never ensued. Therefore, I would like to thank the Missouri Department of Natural Resources, Ameren and Aquila for making this project possible.

Table of Contents

Acknowledgments	ii
List of Figures	vi
List of Tables	xi
Abstract	xiii
Chapter 1 Introduction	1
1.1 Statement of Thesis	3
1.2 Objectives	4
Chapter 2 Background	5
2.1 Basic Wind Energy	5
2.1.1 Turbulent Mixing	8
2.1.2 Surface Roughness	11
2.1.3 Diurnal Variation	14
2.1.4 Low Level Jet	15
2.2 Wind Profilers	20
2.3 Previous work	25
2.3.1 Lamar Low-Level Jet Program	26
2.3.2 Additional Tall Tower Studies Performed in the Great Plains ..	27

2.3.3 Known Errors in Tall Tower Siting and Instrumentation	32
2.3.4 Relating Previous Work to the Current Study	34
Chapter 3 Data and Methodology	36
3.1 Wind Energy Resource Map of Missouri	36
3.2 Tall Tower Data	39
3.2.1 Tower Selection	40
3.2.2 Tower Set-Up	43
3.2.3 Instrumentation Specifics	44
3.2.4 Analysis of Tower Data	46
3.3 Wind Profiler Data	49
3.3.1 Analysis of Wind Profiler Data	50
Chapter 4 Results and Discussion	52
4.1 Results	52
4.1.1 Verification of Current Wind Maps	52
4.1.2 Diurnal Variation	56
4.1.3 The Use of Profiler Winds as a Proxy for Surface Winds	66
4.1.4 Locating the Low Level Jet	73

Chapter 5 Conclusions and Future Directions	88
5.1 Conclusions	88
5.1.1 Verification of Current Wind Maps	88
5.1.2 Diurnal Variation	89
5.1.3 The Use of Profiler Winds as a Proxy for Surface Winds	89
5.1.4 Locating the Low Level Jet	90
5.2 Future Directions	90
References	92

List of Figures

		Page
Figure 2.1	This chart taken from the Wangara experiment demonstrates the typical diurnal variations that occur at different heights in the atmosphere (from Arya, 1998).	15
Figure 2.2	Wind profile demonstrating the structure of the low-level jet. The jet maximum is most noticeably present at 350 ft (from Portman, 2004).	18
Figure 2.3	Typical wind profiler beam configuration consisting of three to five beams: one vertical and two or four tilted near 15° from the zenith in orthogonal directions. Also shows low and high mode range reproduced from NOAA, 2005.	21
Figure 2.4	Diurnal wind speed for three towers located in Kansas (from Schwartz and Elliot, 2005).	28
Figure 2.5	Diurnal wind speeds taken from three towers in Indiana (from Schwartz and Elliot, 2005).	29
Figure 2.6	Diurnal wind speeds taken from three towers located in Minnesota (from Schwartz and Elliot, 2005).	30
Figure 3.1	The green stars indicate the locations of the tall towers equipped, while the yellow star represents the location of the wind profiler the tower data was compared with (AWS Truewind, 2005).	41
Figure 3.2	An image of the Miami tower. The equipment installed can be clearly distinguished at the three heights on the tower.	42
Figure 3.3	An image of the wind vane equipped on each observational tower provided by the NRG Systems Specifications Report.	44
Figure 3.4	An image of the anemometer placed on each observational tower provided by the NRG Systems Specifications Report.	45

Figure 4.1	Diurnal variation plots for the Blanchard Tower. The blue solid line represents Channel 1, the blue dashed line is Channel 2, the green solid line is Channel 3, the green dashed line is Channel 4, the red solid line is Channel 5 and the red dashed line is Channel 6.	56
Figure 4.2	Diurnal variation plots for the Chillicothe tower. The blue solid line represents Channel 1, the blue dashed line is Channel 2, the green solid line is Channel 3, the green dashed line is Channel 4, the red solid line is Channel 5 and the red dashed line is Channel 6.	57
Figure 4.3	Diurnal variation plots for the Maryville tower. The blue solid line represents Channel 1, the blue dashed line is Channel 2, the green solid line is Channel 3, the green dashed line is Channel 4, the red solid line is Channel 5 and the red dashed line is Channel 6.	58
Figure 4.4	Diurnal variation plots for the Miami tower. The blue solid line represents Channel 1, the blue dashed line is Channel 2, the green solid line is Channel 3, the green dashed line is Channel 4, the red solid line is Channel 5 and the red dashed line is Channel 6.	60
Figure 4.5	Diurnal variation plots for the Raytown tower. The blue solid line represents Channel 1, the blue dashed line is Channel 2, the green solid line is Channel 3, the green dashed line is Channel 4, the red solid line is Channel 5 and the red dashed line is Channel 6.	61
Figure 4.6	The variation of wind speed with time for the month of November, 2006 at the Maryville site. The wind profiler wind speed measurements are shown in blue and the observed tower winds for channel 6 are shown in red.	63
Figure 4.7	The variation of wind speed with time for the month of November, 2006 at the Maryville site. The wind profiler wind speed measurements are shown in blue and the observed tower winds for channel 6 are shown in red.	64
Figure 4.8	The variation of wind speed with time for the month of February, 2007 at the Maryville site. The wind profiler wind speed measurements are shown in blue and the observed tower winds for channel 6 are shown in red.	64

Figure 4.9	The wind profiler wind speed at 500 m is plotted against the wind speed from channel 3 of the Raytown tower, both for the month of November.	66
Figure 4.10	The wind profiler wind speed is plotted against the wind speed from channel 3 of the Chillicothe tower, both for the month of November.	66
Figure 4.11	The wind profiler wind speed at 500 m is plotted against the wind speed from channel 3 of the Blanchard tower, both for the month of November.	67
Figure 4.12	The wind profiler wind speed at 500 m is plotted against the wind speed from channel 3 of the Maryville tower, both for the month of November.	67
Figure 4.13	The wind profiler wind speed at 500 m is plotted against the wind speed from channel 3 of the Miami tower, both for the month of November.	68
Figure 4.14	Wind profile for a case where a low-level jet is not present.	73
Figure 4.15	The wind profile when the low-level jet is above 500 m. BLH is the height of the boundary layer.	73
Figure 4.16	The low-level jet is located completely above the 100-m tower height, but intersects the 500-m level. BLH is the height of the boundary layer.	74
Figure 4.17	The low-level jet is located completely below the 500-m height, but is present at the 100-m level. BLH is the height of the boundary layer.	74
Figure 4.18	Extrapolated tower winds to 500 m versus profiler winds at 500 m. The solid red line is the average and the dashed red lines are the average plus or minus the standard deviation. This case shows an occurrence of good correlation since most of the data points are within the standard deviation range.	76
Figure 4.19	Extrapolated tower winds to 500 m versus profiler winds at 500 m. The solid red line is the average and the dashed red lines are the average plus or minus the standard deviation. This case has more incidences of the LLJ being present higher up, nearer to 500 m, because the number of	76

outliers below the standard deviation line exceeds the number above.

- Figure 4.20 Extrapolated tower winds to 500 m versus profiler winds at 500 m. The solid red line is the average and the dashed red lines are the average plus or minus the standard deviation. This case shows a higher incidence of a LLJ being present at 100 m and completely below 500 m since the number of outliers above the standard deviation line exceeds the number below. 77
- Figure 4.21 The percentage of low LLJ occurrences for each month is presented. The percentage was obtained by dividing the number of low LLJ occurrences by the number of data points for each month. 79
- Figure 4.22 The percentage of high LLJ occurrences for each month is presented. The percentage was obtained by dividing the number of high LLJ occurrences by the number of data points for each month. 80
- Figure 4.23 Displayed are the times the high LLJ is detected and the wind speed present at the time of detection for the month of September. The blue line represents the data from the Maryville tower, the red line is for the Blanchard tower data, the magenta line is the Miami data and the cyan line is the Raytown data. 82
- Figure 4.24 Displayed are the times the high LLJ is detected and the wind speed present at the time of detection for the month of December. The blue line represents the data from the Maryville tower, the red line is for the Blanchard tower data, the green line is the Chillicothe data, the magenta line is the Miami data and the cyan line is the Raytown data. 82
- Figure 4.25 Displayed are the times the high LLJ is detected and the wind speed present at the time of detection for the month of March. The blue line represents the data from the Maryville tower, the red line is for the Blanchard tower data, the green line is the Chillicothe data, the magenta line is the Miami data and the cyan line is the Raytown data. 83
- Figure 4.26 Displayed are the times the low LLJ is detected and the wind speed present at the time of detection for the month of September. The blue line represents the data from the Maryville tower, the red line is for the Blanchard tower 83

data, the magenta line is the Miami data and the cyan line is the Raytown data.

Figure 4.27 Displayed are the times the low LLJ is detected and the wind speed present at the time of detection for the month of December. The blue line represents the data from the Maryville tower, the red line is for the Blanchard tower data, the green line is the Chillicothe data, the magenta line is the Miami data and the cyan line is the Raytown data. 84

Figure 4.28 Displayed are the times the low LLJ is detected and the wind speed present at the time of detection for the month of March. The blue line represents the data from the Maryville tower, the red line is for the Blanchard tower data, the green line is the Chillicothe data, the magenta line is the Miami data and the cyan line is the Raytown data. 84

List of Tables

		Page
Table 3.1	Provides the roughness length for the dominant land cover types (Brower, 2005).	36
Table 3.2	Tower Information including latitude, longitude, the elevation at the site, the tower height and the total height above mean sea level are provided.	40
Table 3.3	Displays the date each tower was equipped with the instruments as well as the heights of the instruments on each channel.	46
Table 3.4	The direction of each tower is provided with regard to the wind profiler in Lathrop, MO and distance of each tower from the profiler is also given.	49
Table 4.1	Displays the 50, 70, and 100 m wind speeds found using the wind map.	51
Table 4.2	Displays each channel's average wind speed throughout the months of operation.	52
Table 4.3	Correlation Coefficients are shown for the Blanchard tower. They display the relationship between 500 m wind speeds taken from the Lathrop, MO wind profiler and the observed tower data for each channel.	69
Table 4.4	Correlation Coefficients are shown for the Chillicothe tower. They display the relationship between 500 m wind speeds taken from the Lathrop, MO wind profiler and the observed tower data for each channel.	69
Table 4.5	Correlation Coefficients are shown for the Maryville tower. They display the relationship between 500 m wind speeds taken from the Lathrop, MO wind profiler and the observed tower data for each channel.	69
Table 4.6	Correlation Coefficients are shown for the Miami tower. They display the relationship between 500 m wind speeds taken from the Lathrop, MO wind profiler and the observed tower data for each channel.	70

Table 4.7	Correlation Coefficients are shown for the Raytown tower. They display the relationship between 500 m wind speeds taken from the Lathrop, MO wind profiler and the observed tower data for each channel.	70
Table 4.8	The correlation coefficient for the relationship between the extrapolated tower wind to 500 m and the profiler wind speed at 500 m. Also given is the standard deviation used to locate the number of outliers and the number of outliers present indicating a high LLJ occurrence (the LLJ is near 500 m) or a low LLJ occurrence (the LLJ is near 100 m).	78

Abstract

With energy needs on the rise and our current energy consumption methods polluting the atmosphere, it is the right time to look at alternative forms of energy production. Six Tall Tower wind observation sites were studied in Northwestern Missouri with a long term goal of determining if Missouri is a good resource for wind energy development. The data set collected through the research period is not lengthy enough to determine if Missouri can sustain wind energy resources, but more data is to be collected to determine this in the future. What can be determined through this data is a validation of the observational data we are collecting along with some interesting effects.

A verification of existing wind maps for the State of Missouri has been performed to assist in the positioning of wind farms. Validation of current wind maps using observational data is of key importance because the observational data is actually coming from the heights at which wind turbines will operate. It has been found that the current wind maps match the observed tower data in a general fashion. Diurnal variations in the wind fields were also studied. Wind speeds at the observed heights were found to be stronger during the nighttime hours and weaker during the daytime, as is expected. Other than this basic finding, seasonal changes in wind speed were observed to discover interesting effects within the tower data. Another aspect to be considered involves pairing tower data with wind profiler data to determine if profiler data can be used as a

proxy for lower level winds. Plots of profiler winds versus tower winds were analyzed to determine a threshold for locating low-level jets (LLJ).

Even with only 8 months of data, the dataset is showing promising results for the development of wind energy resources in Northwestern Missouri. This was shown through the average wind speeds found in the diurnal variation plots. In extrapolating the upper-level winds, 500 m, downward to 100 m we found that the correlation produced was not impressive and that it would be best to continue with the standard of using surface winds to estimate upper-level winds. The LLJ was found to occur regularly and frequently. Times were located at which all the towers corresponded well, indicating the presence of a LLJ. Future research will further test if this method is actually detecting the LLJ by finding times when the LLJ is known to be present and comparing those with the times found through our detection method.

Chapter 1 Introduction

The objective of this study is to investigate the wind resource in the state of Missouri to learn about the available wind resource and the factors that influence it. This is a necessary objective for three main reasons: (1) A cleaner form of energy is needed to take the place of the present form of energy production; (2) Wind energy is renewable as opposed to fossil fuels; (3) A local source of energy would help to lessen the cost of energy production and decrease our dependence on foreign countries.

Currently, more than half of all the electricity that is used in the United States is generated from burning coal, and thus large amounts of toxic metals, air pollutants and greenhouse gases are emitted into the atmosphere. Development of just 10% of the wind potential in the 10 windiest states would produce more than enough energy to displace emissions from the nation's coal power plants and eliminate the major source of acid rain in the United States, reduce total emissions of carbon dioxide in the United States by almost a third and world emissions of CO₂ by 4%. If wind energy were to produce 20% of the United State's electricity it could displace more than a third of the emissions from coal power plants, or all of the radioactive waste and water pollution from nuclear power plants (AWEA, 2003).

This is a very realistic and achievable goal considering current technology. The fossil fuels such as coal and petroleum (oil and natural gas) are also of a limited supply and are generally obtained from sources outside of the United

States. If a local, sustainable energy source were found, it would be a strong benefit not only on the state level, but to our country as a whole. Since the wind is a natural, renewable resource that can be harvested to produce electricity at a cost that does not vary significantly with time it would be a good economic alternative to foreign obtained fossil fuels. Furthermore, wind power generation has little negative impact on the environment, making it one of the preferred choices in locations, where the wind conditions are favorable (Blackler and Iqbal, 2005).

With many states beginning to produce wind energy, the question becomes "Why not Missouri?" There should be resources available in Missouri as our neighbors Kansas, Iowa, and even Illinois have shown in their production and use of wind energy is viable. Thus, this research project was conducted in order to investigate wind patterns to discover both some interesting effects, but also as a test of the feasibility of the development of wind energy resources in the State of Missouri. The data set collected through the research period is not lengthy enough to determine if Missouri can sustain wind energy resources, but more data is to be collected to determine this in the future. What can be determined through this data is the verification of existing wind maps for the State of Missouri to assist in the positioning of wind farms. The second part of our research deals with diurnal variations in the wind fields. Detection of the low-level jet, a common phenomenon in the Midwest, will also be attempted as it would significantly impact the amount of wind energy available. The final element to be addressed involves pairing tower data with profiler data to

determine if profiler data can be used as a proxy for lower level winds. Learning more about these aspects of wind energy production will allow us to find out more about sustainable wind energy resources in Missouri and help to determine if site locations will be efficient.

1.1 Statement of Thesis

The current wind maps will be verified through actual measurements of the wind speed and direction taken from (pre)-existing towers across Northwestern Missouri. Since the current wind maps give average wind speeds for heights of 30, 50, 70 and 100m above ground level (AGL) the wind vanes and anemometers used in this study were placed as close to the latter two heights as possible in order to compare the two data sets. Once the wind maps are verified using the tower data it will be possible to determine the areas in Missouri that are most suitable for the farming of wind energy. Validation of current wind maps using observational data is important because the observational data is actually coming from the heights at which wind turbines will operate. It is hypothesized that the current wind maps will match our findings in a general fashion. This study will also look into the diurnal variations in the wind to see if a pattern is distinguishable. It is hypothesized that the winds will be stronger during the nighttime hours and weaker during the daytime. Other than this basic assumption, we are looking to find interesting effects using the tower data. Considering data has been collected while the season is changing from summer

to fall, fall to winter and winter to spring, there may be variations in peak wind speeds and peak times. Any changes of this nature would be helpful information for wind energy farms. Then data from a wind profiler will be compared to the tall-tower data to determine if the profiler data can be extrapolated down to the surface and used as an estimate of surface winds. The low-level jet will also be discussed, and a method of identifying the occurrence of the low-level jet will be employed. It is hypothesized that the low-level jet will be located low enough to influence wind energy production in Northwestern Missouri.

1.2 Objectives

The objectives of this study are;

- (i) to verify the current wind maps,
- (ii) to observe the diurnal variation of wind speed in order to determine if it follows a periodic cycle,
- (iii) to determine if winds from a wind profiler can be used as a proxy for near-surface winds, and
- (iv) to determine a threshold for locating the low-level jet using extrapolated surface wind speeds and wind profiler wind speeds.

Chapter 2 Background

2.1 Basic Wind Energy

In order to better understand wind energy we must look at the processes and actions that influence the wind and wind patterns. Wind is created primarily due to uneven heating of the earth by the sun. The heat absorbed by the surface of the earth is transferred to the air, where it causes differences in air temperature, density and pressure. These differences give rise to forces that move the air throughout the atmosphere. The balance of these forces on the large-scale can produce features such as the trade winds, which are driven ultimately by the temperature difference between the equator and poles. Small-scale forcings such as local temperature differences between land and sea also affect the wind. The earth's rotation, local topographical features and the roughness of terrain all influence the wind's speed and direction.

In particular, the earth's rotation or Coriolis force impacts large-scale circulation patterns. The geostrophic wind occurs when the Coriolis force exactly balances the horizontal pressure gradient force. The wind is not geostrophically balanced near the surface, and this balance is usually not found until an altitude above 1000 m AGL. The equation for the speed of the geostrophic wind is given in natural coordinates as:

$$V_g = \frac{g}{f} \frac{\partial z}{\partial n} \quad (2.1)$$

where V_g is the geostrophic wind, g the acceleration of gravity, f the Coriolis parameter, and $\partial z/\partial n$ is the slope of the isobaric surface normal to the contour lines to the left of the direction of motion in the Northern Hemisphere and to the right in the Southern Hemisphere. The geostrophic wind is thus directed along the contour lines on a constant-pressure surface (or along the isobars in a geopotential surface) with low elevations (or low pressure) to the left in the Northern Hemisphere and to the right in the Southern Hemisphere. This relation between contours and wind is the Buys-Ballot rule (see Djuric, 1994, for example). The geostrophic wind can also be broken down into two scalar components in cartesian coordinates:

$$u = -\frac{g}{f} \frac{\partial z}{\partial y} \quad (2.2)$$

$$v = \frac{g}{f} \frac{\partial z}{\partial x} \quad (2.3)$$

Where u is the east-west component of the wind and v represents the north-south component of the wind field. The geostrophic wind is normally roughly equal to the wind vector (Djuric, 1994). The wind vector is then:

$$V \approx \frac{g}{f} \left| \frac{\partial z}{\partial n} \right| \quad (2.4)$$

The relationship is then expressed mathematically as:

$$V \approx V_g \quad (2.5)$$

This approximation does not hold true near the equator where the Coriolis force disappears. The validity of the geostrophic approximation depends upon the particular context of its use. The geostrophic wind does not take into account the

frictional force, acceleration, curvature of contours or wind speed and direction. These factors are irrelevant for describing geostrophic wind, since they have not been used in its determination (Djuric, 1994).

The geostrophic winds are largely driven by temperature differences, and thus pressure differences, and are not very much influenced by the surface of the earth. In this study we are more concerned with the boundary layer which is the layer of air directly above the earth's surface. The layer extends to about 100 m above the ground on a clear night with low wind speeds, and up to more than 2 km on a fine summer day (Petersen *et al.*, 1998a). The surface layer, or lowest 10% of the boundary layer depth, is very much influenced by the interaction of the atmosphere with the ground surface. The wind will be slowed down by the earth's surface roughness and obstacles. Roughness features such as forests or fields of crops slow the wind to different degrees. Obstacles to the wind such as buildings, or rock formations can decrease wind speeds significantly, and they often create turbulence in their vicinity. The geostrophic approximation will not work for surface winds since the approximation does not take into account these influential surface features. Wind directions near the surface will be slightly different from the direction of the geostrophic wind because of the frictional force (Danish Wind Industry Association, 2003). Thus, the geostrophic drag law is thought to give a better representation of the wind speed near the surface. The geostrophic drag law is represented by the equation:

$$V_g = \frac{u_*}{\kappa} \sqrt{\left[\ln\left(\frac{u_*}{fz_0}\right) - A \right]^2 + B^2} \quad (2.6)$$

where u_* is the friction velocity, κ the von Karman constant, z_0 is the roughness length and A and B are dimensionless functions of stability. The friction velocity is a reference wind velocity applied to motion near the ground where the shearing stress is often assumed to be independent of height and approximately proportional to the square of the mean velocity. The von Karman constant is an empirical constant that characterizes the dimensionless wind shear for statically neutral conditions and has a value of 0.4. Then, the roughness length parameter is the height above the displacement plane at which the mean wind becomes zero when extrapolating the logarithmic wind-speed profile downward through the surface layer (AMS, 2007). This modified form of the geostrophic wind does account for surface roughness features and can take into account the terrain and the stability of the atmosphere, but caution must still be taken as not all wind climates near the ground are determined by the winds aloft.

2.1.1 Turbulent Mixing

To discuss turbulent mixing, turbulence must first be defined. According to Arya (1998), the general characteristics of turbulence are as follows:

1. Irregularity or randomness: This makes any turbulent motion essentially unpredictable or chaotic. No matter how carefully the conditions of an experiment are reproduced, each realization of the flow is different and cannot be predicted in detail. The same is true of the numerical simulations (based on Navier-Stokes equations), which are found to be

highly sensitive to even minute changes in initial and boundary conditions. This is known as sensitive dependence on initial conditions (SDIC). For this reason, a statistical description of turbulence is invariably used in practice.

2. Three-dimensionality and rotationality: The velocity field in any turbulent flow is three-dimensional (excluding the so-called two-dimensional or geostrophic turbulence, which includes all large-scale atmospheric motions) and highly variable in time and space. Consequently, the vorticity field is also three-dimensional and flow is highly rotational.
3. Diffusivity, or ability to mix properties: This is probably the most important property so far as applications are concerned. It is responsible for the efficient diffusion of momentum, heat, and mass (e.g., water vapor, CO₂, and various pollutants) in turbulent flows. The macroscale diffusivity of turbulence is usually many orders of magnitude larger than the molecular diffusivity. The former is a property of the flow regime while the latter is a property of the particular fluid. Turbulent diffusivity is largely responsible for the evaporation in the atmosphere, as well as for the spread (dispersion) of pollutants released in the atmospheric boundary layer. It could be responsible for increased resistance and friction around wind turbines.
4. Dissipativeness: The kinetic energy of turbulent motion is continuously dissipated (converted into internal energy or heat) by viscosity. Therefore,

in order to maintain turbulent motion, the energy has to be supplied continuously. If no energy is supplied, turbulence decays rapidly.

5. Multiplicity of scales of motion: All turbulent flows are characterized by a wide range (depending on the Reynolds number) of scales or eddies lengths. The transfer of energy from the mean flow into turbulence occurs at the upper end of scales (large eddies), while the viscous dissipation of turbulent energy occurs at the lower end (small eddies). Consequently, there is a continuous transfer of energy from the largest to the smallest scales. Actually, it trickles down through the whole spectrum of scales or eddies in the form of a cascade process. The energy transfer processes in turbulent flows are highly nonlinear and are not well understood.

Therefore turbulence is a flow that is not smooth or regular. Turbulence is apparently chaotic by nature or irregular. The turbulence intensity is a measure of the overall level of turbulence and can be found using the equation:

$$I = \frac{\sigma}{\bar{U}} \quad (2.7)$$

where σ is the standard deviation of wind speed variations about the mean wind speed \bar{U} , usually defined over 10 min or 1 hour (Bossanyi *et al.*, 2001). Turbulence dominates as the vertical transport mechanism in the boundary layer. Vertical transport then results in the mixing of a layer. In a convective boundary layer, buoyancy-driven thermals constantly overturn the air, keeping the layer well mixed and profiles of conserved variables approximately uniform with height (Lock, 2000).

Turbulent mixing is due to surface friction, solar heating and evaporation. Turbulent mixing is most typically observed near the middle of the day when rising warm air has reached the top of the planetary boundary layer. As the air rises, it loses moisture and clouds form. Colder, drier air comes down to replace the rising air. If enough air is circulating, it generates turbulent mixing, which can generate an atmospheric mixed layer from the earth's surface to a height of over a kilometer. It is during this time of day that winds are also at their peak speeds in the lower levels as there is a substantial temperature difference between the surface and the upper-levels in the atmosphere. Thus, it has been shown that increasing wind speeds will increase turbulent fluxes which enhance vertical mixing.

2.1.2 Surface Roughness

Surface roughness is a term that refers to the features present on the surface and their effect on the wind flow. Trees, ground cover, hills, snowfall and buildings all contribute to the surface roughness. These features serve as a sink for turbulent flow due to the generation of drag forces and increased vertical wind shear. In micrometeorology, the surface roughness is typically measured by the roughness length. The roughness length is a length scale that arises as an integration constant in the derivation of the logarithmic wind profile relation. In neutral stability the logarithmic wind profile extrapolates to zero wind velocity at a height equal to the surface roughness length (AMS, 2007). The aerodynamic

roughness of a flat and uniform surface may be characterized by the average height of the various roughness elements, their aerial density, characteristic shapes, and dynamic response characteristics (e.g. flexibility and mobility). These characteristics would be important if one were interested in the complex flow field within the roughness canopy or layer, but there is not much hope for a generalized and simple theoretical description of such a three-dimensional flow field in which turbulence dominates over the mean motions (Arya, 1998). The surface roughness is then characterized by only one or two roughness characteristics in the surface layer to simplify the flow field. These characteristics can be empirically determined from wind-profile observations.

The roughness length parameter is the first of these characteristics. The roughness length parameter can be determined, in practice, from the least-square fitting of the equation:

$$\frac{U}{u_*} = \frac{1}{\kappa} \ln\left(\frac{z}{z_0}\right) \quad (2.8)$$

through the wind profile data. Where U is the wind speed at height z and the roughness length parameter is unitless. The roughness length parameter is the height above the displacement plane at which the mean wind becomes zero when extrapolating the logarithmic wind-speed profile downward through the surface layer (AMS, 2007). Literally, the roughness length is the height above the surface at which the mean wind speed is zero due to the surface features. Graphically, the roughness length parameter can be found by plotting $\ln(z)$ versus U and extrapolating the best-fitted straight line down to the level where $U = 0$. The intercept on the ordinate axis must be $\ln(z_0)$. This procedure is unable

to describe the actual wind profile below the tops of roughness elements. Empirical estimates of the roughness parameter for various natural surfaces can be arranged according to the type of terrain or the average height of the roughness elements. For example forests would have a greater roughness length than a field of cut grass.

The displacement height is the second characteristic. For very rough and undulating surfaces, the soil-air or water-air interface may not be the most fitting reference point for measuring heights in the surface layer. The air flow above the tops of roughness features is dynamically influenced by the ground surface as well as by individual roughness elements (Arya, 1998). Therefore, it may be suggested that the appropriate reference point can be found somewhere between the earth's surface and the tops of roughness features. In practice, the reference point is established empirically from wind-profile measurements in the surface layer under near-neutral stability conditions. The modified logarithmic wind-profile law used for this purpose is:

$$\frac{U}{u_*} = \frac{1}{\kappa} \ln \left(\frac{z' - d_0}{z_0} \right) \quad (2.9)$$

In which d_0 is the displacement height and z' is the height measured above ground level. The displacement height may be expected to increase with increasing roughness density and approach a value close to the average height of the various roughness elements for very dense canopies in which the flow within the canopy might become stagnant, or independent of the air flow above the canopy (Arya, 1998). Thus it is important to keep in mind how surface features can affect the wind flow.

2.1.3 Diurnal Variations

Being that the wind is primarily due to uneven solar heating of the surface, it makes sense that wind speeds would have a fundamental pattern on a daily basis. Based on this concept, wind speeds would decrease during the evening hours when there is no solar heating and increase in the daytime when solar heating is at its maximum. The interpretation of wind profiles in a day to day manner may not represent the true diurnal variations due to changing synoptic conditions and variations in the surface energy balance. But, when the profiles are averaged over a period of time, such as a month or longer, the diurnal variations can be seen. This is shown in Figure 2.1 from Arya (1998) where a tower near Oklahoma City, OK was equipped with instruments to measure wind speed for a period of one year. Figure 2.1 confirms the hypothesis that wind speeds are generally stronger in the daytime as opposed to the evening hours, but just for the levels closest to the surface. This is the case because the surface is more susceptible to energy transfer from the sun. Once the surface heats up with the sun there is a more rapid and efficient transfer of momentum from aloft through the evolving unstable planetary boundary layer in the daytime. In the levels above 98 m winds are actually stronger in the evening hours and the diurnal wave is 180° out of phase. This is important to note as wind turbines are now being placed near 100 m because stronger winds are found further up in the planetary boundary layer. As a wind developer it is important to know when to

expect peak winds and, for a basic first assumption the, diurnal pattern makes for a good start.

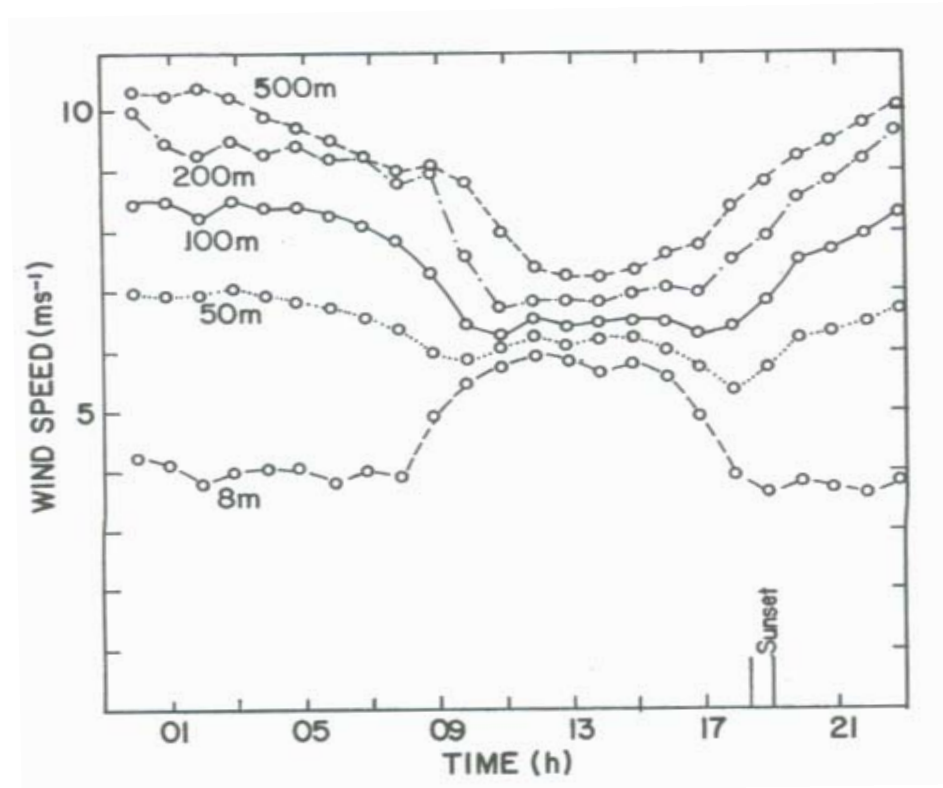


Figure 2.1. This chart taken from the Wangara experiment demonstrates the typical diurnal variations that occur at different heights in the atmosphere (adapted from Arya, 1998).

2.1.4 Low Level Jet

The low-level jet (LLJ) is a common phenomenon in forecasting for the Great Plains and Eastern United States. As the name implies, it is a fast moving band of air in the low levels of the atmosphere. It can rapidly transport Gulf moisture and warmer temperatures to the North at speeds ranging from 12 to over 35 m/s. There are two primary classifications of low-level jets. They are the

nocturnal LLJ and the mid-latitude cyclone induced LLJ. The nocturnal LLJ will be focused on in this study since it is easily detectable through diurnal variations of wind speed. This regularity of the nocturnal LLJ also means that it has a predictable impact on the availability of the wind energy resource.

The nocturnal LLJ is strongest in the early morning hours and decreases during the day due to a reverse in the east to west temperature or density gradient since humidity does play a role in the development. The reverse in the temperature gradient is caused by warming of surface air. Air closer to the surface will warm more quickly than air further aloft during the day. The air at the 850-mb level cools and warms more quickly than that at the same level further to the east because the western Great Plains is at a higher elevation. Air is generally colder to the west due to surface radiational cooling of the ground and a drier climate. The cooling of high elevation air relative to the air at the same geopotential height further east causes a pressure gradient to flow from warmer east air toward the cooler western air. The nocturnal LLJ then forms as the release of daytime convective turbulent stresses allow nighttime winds to accelerate to supergeostrophic wind speeds above a stable boundary layer. When surface winds of less than 5 m/s are present, wind speeds found at an altitude of 100 m can be greater than 20 m/s due to the nocturnal LLJ (Lundquist, 2005).

The acceleration of the wind speed causes the higher winds above the ground to separate or decouple from the air nearer the surface while increasing the wind shear, or the rate of change of wind speed with height. The turbulence

generated by this wind shear can induce nocturnal mixing events and control surface-atmosphere exchange, affecting atmospheric transport and dispersion. The Coriolis force turns easterly flowing parcels to the right of the path of motion giving the LLJ a strong southerly component.

In studying the LLJ phenomenon, Blackadar (1957) found significant occurrences of maximum wind speed occurring below 1500 m above the ground. This maximum wind speed occurs most frequently during the night and is most strongly developed around 0300 local time. The wind profile showed a rapid increase of wind with height to a maximum, which in the best examples exceeded 25 m/s, then a more or less rapid decrease at higher levels (Pitchford and London, 1961). The jet generally formed over a 3-h transition period after sunset, with the jet speed often reaching several temporal maxima at 3-5 h intervals through the night. It was also found to apparently follow the local terrain (Pichugina *et al.*, 2004). A nocturnal low-level jet wind profile is shown in Figure 2.2. It was measured with a pibal before sunrise during a hot-air balloon competition at Battle Creek, MI, in June 1989. The profile shows a maximum of about 26 knots at 350 ft. The wind speed increases, from less than 5 knots near the surface, to the 350 ft maximum and then decreases to about 13 knots near 1150 ft (Portman, 2004).

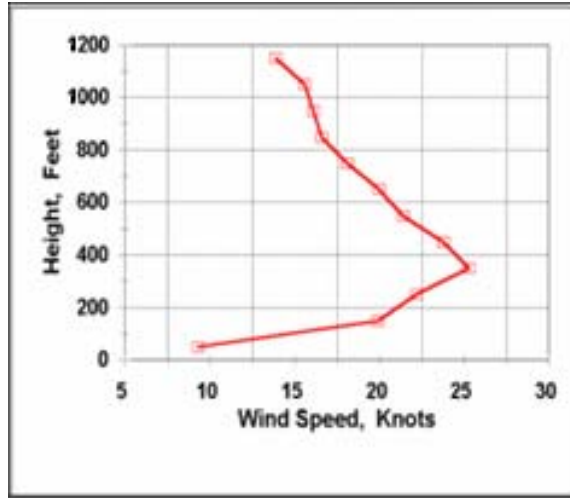


Figure 2.2. Wind profile demonstrating the structure of the low-level jet. The jet maximum is most noticeably present at 350 ft (adapted from Portman, 2004).

Once the evening decoupling process is completed, the mixing intensity is more dependent on larger-scale controls than on details of near-surface turbulence parameterizations. On the larger-scale, accurate prediction of LLJ speed requires proper representation of the ageostrophic wind profile at sunset and proper representation of the stabilization process, including the decoupling of the flow from surface friction during the early evening transitional period (Banta *et al.*, 2006). The nocturnal LLJ has a role in generating shear and turbulence between the level of maximum wind speed and the earth's surface, and thus can strongly influence surface-atmosphere exchange at night (Pichugina *et al.*, 2004). The shear generated is often an important source of turbulence and turbulent fluxes in the nighttime boundary layer.

The formation of LLJs during nighttime is very important for wind energy operations. LLJs provide enhanced wind speeds to drive the turbines. However, one issue is the unfortunate failure of turbine hardware as a result of significant

nocturnal bursts of turbulence (Banta *et al.*, 2006). Jets with speed maxima above 10 m/s that occurred at very low levels could be potentially damaging to wind turbines (Pichugina *et al.*, 2004). This analysis indicated that the highest wind speeds were associated with the smallest gradient Richardson numbers (Ri), as expected. The gradient Richardson number provides a measure of the intensity of mixing or turbulence present and is a simple criterion for determining the presence or absence of turbulence in a stably stratified environment. The Richardson number is determined using the equation:

$$Ri = \frac{g}{T_v} \frac{\partial \Theta_v}{\partial z} \left| \frac{\partial V}{\partial z} \right|^{-2} \quad (2.10)$$

where T_v is the virtual temperature, Θ_v is the virtual potential temperature, $\frac{g}{T_v} \frac{\partial \Theta_v}{\partial z}$ is the static stability parameter and V is the actual wind vector. The static stability parameter is a measure of buoyant accelerations or forces on air parcels. Thus, Ri is found to be a dimensionless ratio of buoyancy production of turbulence to shear production of turbulence, and it is used to indicate dynamic stability along with the formation of turbulence. A large positive value of $Ri > 0.25$ indicates weak and decaying turbulence or a completely nonturbulent environment, while a value of $Ri < 0.25$ indicates dynamically unstable and turbulent flow (Arya, 1998). The condition $Ri < 0.25$ was true for all nights with high wind speeds. As is discussed in Kelley *et al.* (2004) it has been found that wind turbines experience high levels of turbulent loading when the gradient Ri calculated over the rotor disk layer is between 0.0 and +0.1, with the largest response often seen with Ri values in the vicinity of +0.01 to +0.02. Thus we

would expect to see some form of a significant structural response in operating wind turbines exposed to these conditions (Banta *et al.*, 2004).

2.2 Wind Profilers

During the last 20 years, Doppler radars have been systematically developed to survey the atmosphere and derive the wind profile from echoes of transmitted radio waves produced by turbulence in clear air. A wind profiler is the operational application of a phased-array radar originally developed for measuring the echo intensity and the wind profile up to about 30 km with height resolutions from 100 to 1500 m. Wind profilers measure the speed and direction of the wind as a function of height (Figure 4 shows the typical wind profiler beam configuration). Wind profilers work by radiating sequences of high power pulses in the vertical and in oblique directions. By analyzing the received echoes, the radial velocity and the turbulence intensity can be computed. Observations from at least three directions are necessary to determine direction and speed of the wind. For this reason there are three- and four-beam wind profiler measurement techniques. The three-beam technique derives the horizontal components of the wind from two orthogonal oblique beams and a vertical beam. The less commonly applied method of the four-beam technique finds the horizontal winds from radial velocities measured with two orthogonal sets of opposing coplanar beams. It has been shown that the four-beam wind profiler technique is more reliable, accurate and precise when compared to the three-beam technique, even

though it is not used as much operationally (Kobayashi *et al.*, 2005). This evaluation concludes that the larger error of the three-beam method is due to the fact that the vertical velocities measured by the vertical antenna beam are not characteristic of the airflow over the area across the beams whenever the vertical airflow has spatial variability (Kobayashi *et al.*, 2005). This finding implies that the four-beam method is less susceptible than the three-beam method to vertical airflow with spatial variability and it is better in measuring horizontal components of the wind.

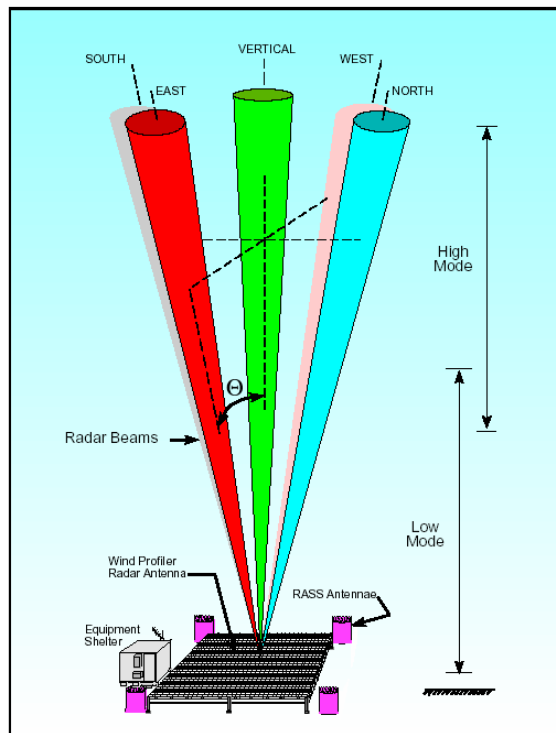


Figure 2.3. Typical wind profiler beam configuration consisting of three to five beams: one vertical and two or four tilted near 15° from the zenith in orthogonal directions. Also shows low and high mode range reproduced from NOAA, 2005.

The measuring capability and performance of any wind profiler is limited by its sensitivity, which improves with higher transmitted power levels and larger

antennae. The maximum reachable height of a wind profiler radar also depends on the operating frequency. To monitor atmospheric processes up to 30 km, 16 km and 5 km, wind profiler systems with operating frequencies at about 50 MHz, 400 MHz and 1000 MHz are used respectively. NOAA (National Atmospheric and Oceanic Administration) is currently using three beam wind profilers in a 404 MHz network with some 449 MHz frequency wind profilers spread throughout. Therefore, the NOAA network would measure winds up to heights of approximately 16-18 km. The NOAA wind profilers use two modes of operation: a low mode that starts at 500 m AGL and goes up to 9250 m AGL and a high mode that starts at 7500 m AGL and goes up to 16250 m AGL. The low and high modes overlap at 8 levels reported between 7500 and 9250 m AGL and the height increment between levels is 250 m for both modes. The FSL (Forecast Systems Laboratory, operated by NOAA) database has a total of 72 levels available within the low and high modes, with a maximum of 64 levels in the integrated profile. When the wind profilers operate in the high mode, a longer transmitted pulse, or increased average power, is used. Therefore, sensitivity in the high mode is increased by a factor of about forty. The returned signal strength is lower at the top of the low mode than it is at the bottom of the high mode thus, all things being equal, the high mode data is probably of better quality. This accounts for the horizontal boundary that is visible in all signal power displays at 7.5 km AGL.

Profiler data can also have problems caused by interfering signals, even with well-designed and properly operating systems at relatively clutter-free sites.

The primary sources of interfering signals are ground and sea clutter, radio frequency interference and atmospheric echoes in radar side lobes. Then, there are also transitory targets that may have very strong echoes, such as aircraft and migrating birds, but whose transitory nature allows profiler data processing to operate adequately.

Wind profilers work in most meteorological conditions, but the data may be suspect in times of severe thunderstorms and when gravity waves are present. This is the case because the averaged radial velocities are representative of the actual mean radial winds in most meteorological conditions. If the mean wind is not horizontally uniform during the averaging time, then the averaged radial velocities may not be representative of the mean radial wind. Meteorological conditions in which short spatial and temporal scales of variability have amplitudes as large as the mean, such as severe storms, limit the use of profilers for measuring horizontal wind profiles (Office of Federal Coordinator of Meteorology (OFCM), 2006). However, even in these cases the radial velocities measured by the profiler may be very accurate even if it is only just for one antenna cycle. The key is to treat the radial velocity profiles independently, and then the data can portray the dynamics of the radial velocity field as long as the sampling interval is suitably short.

Another condition that can cause the local horizontal wind uniformity assumption to be invalid is the presence of gravity waves. The vertical velocity measured by the zenith beam can be very different from the vertical velocity at the oblique resolution volumes, and if the waves are standing waves, temporal

averaging will not reduce the difference. The gravity waves of most concern are those with spatial scales less than the resolution volume separation and temporal scales longer than the profiler averaging time (OFCM, 2006). The extent of problems caused by gravity waves in profiler data is unknown, but gravity waves with amplitudes large enough to cause errors are not uncommon.

Wind profilers can measure winds many kilometers from the ground and they sample winds almost continuously. The winds are measured nearly directly above the site and both the horizontal and the vertical air velocity can be measured. Wind Profilers have a high temporal and spatial resolution although the cost per observation is low because they operate unattended in pretty much all weather conditions. Wind profilers can also operate in high wind and in high acoustic noise environments. Since wind profilers can be adapted to measure temperature profiles up to 5 km when they are used in conjunction with a Radio-Acoustic Sounding System (RASS), there is the possibility to obtain temperatures profiles at a frequent rate.

Wind profiler radars provide wind measurements and turbulence information as a function of altitude in most weather conditions; therefore they have the ability to be put to many uses. The region of observations of the wind profilers also ranges from the surface up to 30 km. The altitude resolution is from 30 m up to 1500 m and the time between profiles ranges from just minutes to an hour, making the wind profiler a very valuable tool.

2.3 Previous Work

Few experiments have been conducted in measuring wind speeds at the heights of 70 m, 100 m and above 100 m. Most wind speed anemometer measurements are at heights of 50 m or lower. A conventional practice in the wind energy industry is to analyze data from shorter towers and extrapolate the data to turbine hub heights for wind farm design and wind energy prediction. However, this technique is much less reliable for hub heights of 80 m and higher (Schwartz and Elliot, 2005). Considering the trend of larger turbines, 80 m and taller, is expected to continue, it seems necessary to actually measure the wind speeds at these heights to better estimate the wind resource. The importance of taking wind measurements at a site can be shown by a common illustration including two wind sites that have the same annual wind speed. One site has a constant wind speed of 10 m/s, while at the other site the wind blows at 20 m/s half of the time and does not blow at all the rest of the time. At the latter site, eight times as much power is available for half of the time. Thus the second site will, over a year's time, provide four times the energy of the first one. The purpose of this example is to demonstrate the general conclusion that any variation in wind speed on a temporal or spatial scale that a particular wind turbine dynamics can respond to will tend to yield more energy than a constant wind of the same annual average (Carlin, 2004).

2.3.1 Lamar Low-Level Jet Program

The objective of the Lamar Low-Level Jet Program (LLLJP) was to characterize the turbulence environment at a representative Great Plains wind resource site at heights in the atmosphere where new designs of low-wind speed turbines will be installed over the next few years. This project is described in full detail by Kelley *et al.* (2004). Of particular interest was the nocturnal low-level jet stream that forms frequently over the Great Plains, mainly during the warmer months. It was a program objective to develop an understanding of the role of the jet in producing lower level shear and turbulence where wind turbines will be operating. To acquire the necessary data to meet the program goals, General Electric Wind Energy installed a 120 m meteorological tower at the site of a planned wind farm development site south of Lamar, Colorado. The National Renewable Energy Laboratory (NREL) equipped the tower with several levels of sensitive instrumentation to measure the turbulence environment. In addition, NREL installed an acoustic wind profiler, or Sound Detection and Ranging Radar (SODAR), nearby to locate and quantify the LLJ seen over the site and correlate that information with the turbulence data collected on the tower. A collaborative program with the NOAA Environmental Research Laboratory was established and a brief field measurement program at the LLLJP Site was executed in early September 2003. This effort employed their high-resolution Doppler Light Detection and Ranging (LIDAR) in combination with the tower-based measurements and the SODAR. The tower mounted instrumentation for this

study included three-axis sonic anemometers installed at heights of 54, 67, 85, and 116 m. Conclusions reached after 1 year of statistical data analysis taken from October 2001 to September 2002 indicate the highest available energy density at the LLLJP Site occurred in late spring and early summer (April through June). The highest turbulence intensities were seen in the warm season (April through September) with the highest mean values found in June and July. The warm season was also dominated by southerly winds in which low-level jets were known to form frequently. Other turbine specific results were obtained along with further investigation of the behavior of the low-level jet phenomenon in response to its potential turbine impacts (Kelley *et al.*, 2004).

2.3.2 Additional Tall Tower Studies Performed in the Great Plains

Physical measurements of parameters such as wind speed, wind power density, and wind speed shear at heights of 80-120 m were practically nonexistent a few years ago and are still rare today (Schwartz and Elliot, 2006). Several studies have recently been conducted at the state level with support from the U.S. Department of Energy. Wind vanes and anemometers were placed on pre-existing tall towers to create a thorough climatology for wind energy development areas in the United States. Measurements of wind characteristics over a wide range of heights up to and above 100 m are useful to: (1) describe the local and regional wind climate; (2) confirm wind resource estimates produced by numerical models; and (3) assess changes in wind characteristics

and wind shear over the area swept by the blades of a turbine (Schwartz and Elliot, 2006). A tall tower wind climatology will better define areas where wind energy production could be feasible, and may even include regions where current 50 m measurements indicate the wind resource may not be sufficient for substantial energy production. Standard graphs of important wind characteristics including annual, monthly and diurnal averages of wind speed and power, frequency of wind speed, and frequency of speed by direction were produced for each measurement level. The Schwartz and Elliot (2005) study focuses on towers instrumented in the states of Kansas, Indiana and Minnesota.

Six tall tower stations were established throughout Kansas. The stations became operational between April and mid June 2003 with five stations having observations through the end of June 2004 and one having observations through early April 2004. The towers were outfitted with anemometers and wind vanes at three levels: 50, 80 and 110 m. The diurnal wind speeds are given for three of the towers in Figure 2.4. It was found that the nocturnal wind speed peaks between 2100 and 2400 Local Standard Time. The diurnal variation pattern shows strong nighttime winds exist and it is noted that the strongest nocturnal southerly winds will probably have the greatest 100-m wind resource. This point emphasizes the control of the low-level jet strength in regard to the available wind energy resource for the state of Kansas. The nocturnal LLJ influences many locations in this region and may have a greater influence on the wind resource at 80-100 m than at 50 m.

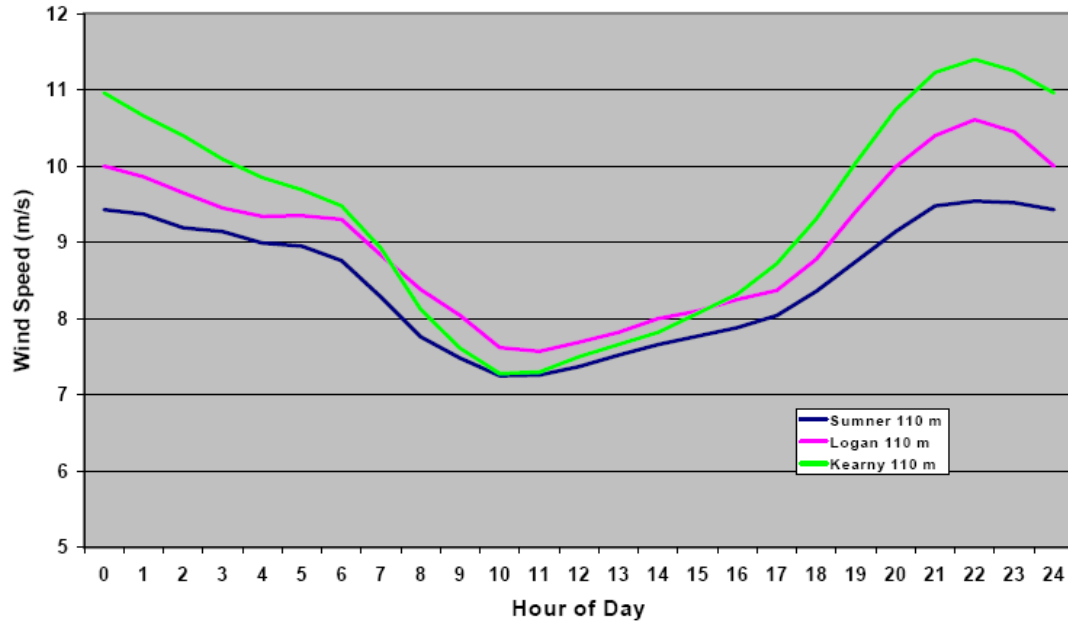


Figure 2.4. Diurnal wind speed for three towers located in Kansas (adapted from Schwartz and Elliot, 2005).

Five tall tower stations were selected in Indiana. The stations have anemometers and wind vanes at three levels: 10, 49, and 99 m above the ground with three stations having measurements for one year. The diurnal wind speed is shown in Figure 2.5. Winter and spring have the greatest resource with peak wind speed generation occurring during this span. Stronger episodes of south-southwest winds during the winter and spring averaged to be 10.5-11.0 m/s for the Goodland, IN site. Annual average wind speeds of 8 m/s and higher for heights of 80-100 m at specific locations generally draw interest from potential wind farm developers.

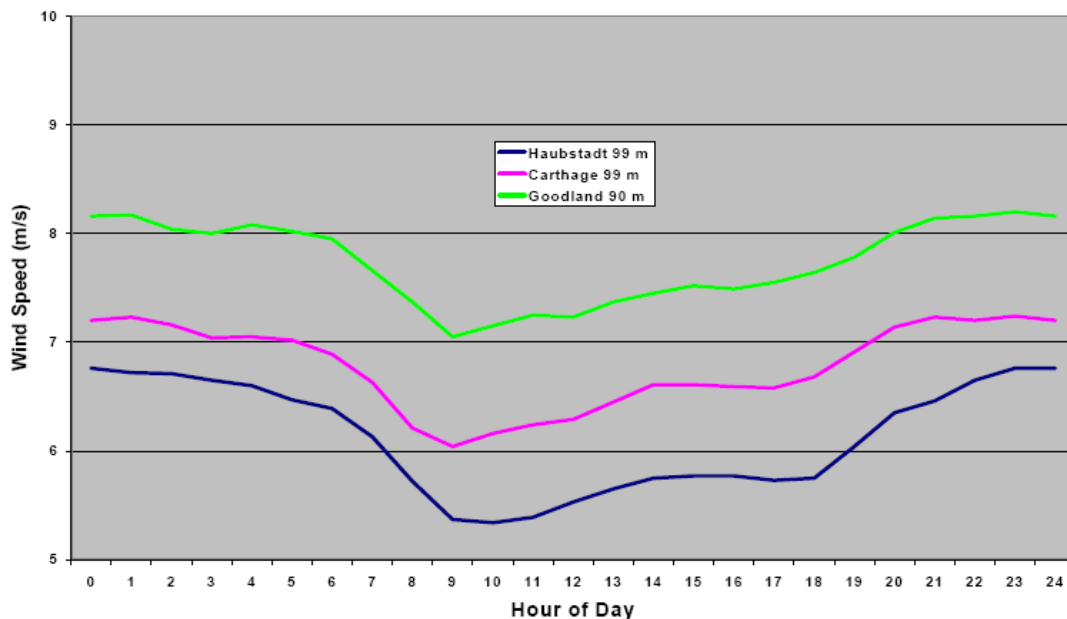


Figure 2.5. Diurnal wind speeds taken from three towers in Indiana (adapted from Schwartz and Elliot, 2005).

Nine tall tower locations were established throughout the State of Minnesota between 1990 and 2004. The highest level at seven of these towers is 90 m, while one tower is 85 m and one other tower has wind data at 120 m. The three towers used for the analysis had anemometers at 30, 60, and 90 m and wind vanes at 30 and 90 m. The year of 2001 to 2002 was chosen for analysis. The diurnal variation is shown in Figure 2.6 for three of the towers included in this study. The results found in this study imply that subregional terrain can cause a significant difference in the wind resource. The land-lake breeze circulation also influences many locations in this area and may have a greater influence on the wind resource at 80-100 m than at 50 m. This is an ongoing project so data is still being collected by these towers.

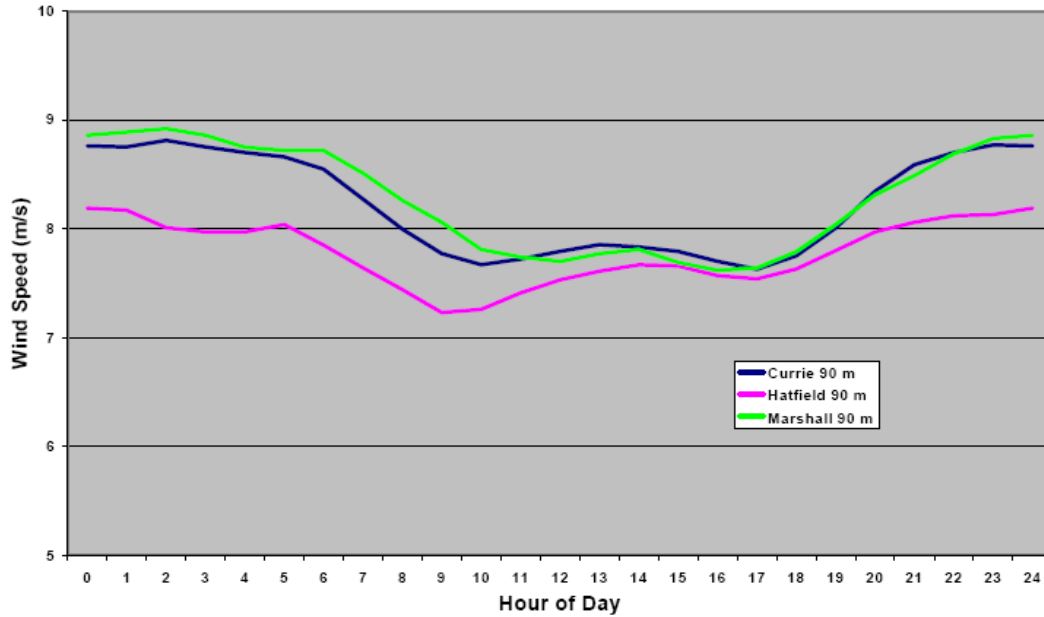


Figure 2.6. Diurnal wind speeds taken from three towers located in Minnesota (adapted from Schwartz and Elliot, 2005).

There are two significant results found from analyzing the data obtained from these tall towers. First of all, the strength of the nocturnal and southerly winds seems to control the wind resource at the different sites. Secondly, the average wind shear exponent of 50-100 m at tall towers in the central United States is influenced by strong southerly winds and is significantly higher than the standard value often used for conservative estimates of the wind resource at the turbine height. In time, tall tower data wind data supplemented by data from remote sensing networks may help us develop a clearer image of wind characteristics at turbine hub heights and allow for a more systematic operation of wind farm power plants to meet our energy needs (Schwartz and Elliot, 2005).

A second study was conducted by Schwartz and Elliot (2006) which focused on the wind shear characteristics at tall tower sites in the Central Plains

of the United States. A total of 13 towers were used for this study. Eleven of the towers had the highest anemometer level between 100 m and 113 m. Two towers had the highest measurement level between 70 m and 85 m above the ground. The division of the towers among the states is: two sites in Texas and Oklahoma; six sites in Kansas; and one site each in Colorado, South Dakota, and North Dakota. The periods-of-record at 12 of the 13 towers were approximately 2 years. This study focused more on wind speed shear measurements to gain knowledge about wind shear characteristics, reduce uncertainty concerning the resource and enhance wind farm design (Schwartz and Elliot, 2006).

2.3.3 Known Errors in Tall Tower Siting and Instrumentation

The wind is highly variable and difficult to predict or forecast, thus making it a difficult parameter to model numerically (Peterson *et al.*, 1998a). Variability is also an intrinsic feature of climate and must be taken into consideration during the siting process. The climate can vary between consecutive decades, but the strongest variations may be year to year due to the El Nino Southern Oscillation (ENSO). Thus, the results presented here can only be interpreted as being representative of the year 2006-2007 for each tower. Significant interannual variations due to ENSO profoundly impact the weather and climatology of mid-Missouri and the Midwest in general (see Lupo *et al.*, 2007, for example). To what extent the period of observation is representative of the longer-term climate

and, more importantly, how large a deviation may be expected in future decades are questions that must be answered and accounted for. A study of climatic variability performed in Northern Europe found that variations in wind energy of up to 30% can be expected from one decade to another (Petersen *et al.*, 1998a). This large variation is probably due to the North Atlantic Oscillation (NAO) which is present in Northern Europe. Interdecadal variations such as the NAO should be considered while assessing a site for wind resource development. Another siting aspect relates to the roughness of the area surrounding the site. The wind resource will be understated if the investigation is based mainly on observations in built-up, high-roughness or otherwise sheltered areas. Conversely, the overall wind resource will be exaggerated if the observations are mainly from low roughness, very exposed areas (Landberg *et al.*, 2003).

Wind speeds can also be falsely represented through errors encountered as a result of the effect of the mast or tower used to support the sensing instruments. The tower or mast on which the anemometer is mounted interferes with the flow and therefore introduces errors in the measured wind speed and direction. For boom-mounted instruments this leads to a reduction in the wind speed measured downwind of the tower, as well as a smaller reduction in the wind speed measured on the upwind side. Although this so-called “tower effect” presents a major problem with regard to the measurement of unbiased wind data, there have been few adequate published investigations of this event. One investigation indicated a slight increase in the ratio of tower to reference values with increasing speed, a maximum ratio of about 1.31 with directions parallel to

the tower side, a retardation of 25-50% in the lee side, and deviations in the wind direction up to 11° (Dabberdt, 1968). While the tower effect has not been rigorously studied it is known to be present as a problematic occurrence in most wind speed studies.

Other errors incurred by instrumentation include that of the anemometer. In general, the sources of error in anemometry include the tower effect, boom and other mounting arrangements, as previously discussed. The anemometer design and its response to the turbulent characteristics of the flow, and the calibration procedure can also introduce error (Peterson *et al.*, 1998b). Clearly, proper maintenance of the anemometer is also important and can reduce the error incurred. In some instances, special problems arise which can be contributed to icing of the sensor or even deterioration of the mechanical parts of the anemometer. It is important to be aware of all known errors so that they can be avoided or accounted for in the data.

2.3.4 Relating Previous Work to the Current Study

Both the Lamar low-level jet project (Kelley *et al.*, 2004) and the studies performed by Schwartz and Elliot (2005; 2006) took observations from similar heights as the study we have performed. Of particular interest with the Lamar project was the nocturnal low-level jet stream which is also studied in our research project. Although, it is said that the summer months are focused on in the LLLJP, we are observing the fall, winter and part of the spring season. The

difference between our project and the LLLJP is that we are trying to detect the low-level jet through extrapolation of the surface wind to the height of 500 m and comparing that with the 500-m profiler wind speed. In the LLLJP the objective was to develop an understanding of the role of the jet in producing lower level shear and turbulence which is something that will not be touched on in our study. As done by the LLLJP and the studies performed by Schwartz and Elliot (2006) we would like to supplement the observational tower data from remote sensing networks to help develop a clearer image of wind characteristics at turbine hub heights and allow for a more systematic operation of wind farm power plants to meet our energy needs.

Chapter 3 Data

3.1 Wind Energy Resource Map of Missouri

The Arc GIS wind map created by AWS Truewind Ltd.- commissioned by the Missouri Department of Natural Resources (DNR)- was made to assist in assessing the potential for wind energy development in Missouri and encouraging developers to find suitable sites for wind energy projects. The Arc GIS maps were created using the MesoMap system. The MesoMap system is comprised of the Mesoscale Atmospheric Simulation System (MASS) and a program called WindMap. The MASS model is a numerical weather model that “simulates the fundamental physics of the atmosphere including conservation of mass, momentum, and energy, as well as the moisture phases, and it contains a turbulent kinetic energy module that accounts for the effects of viscosity and thermal stability on wind shear”(Brower, 2005). The MASS model has high computational demands since it can simulate the evolution of atmospheric conditions in the time frame of a few seconds. Thus, it is necessary to couple the MASS model with a simpler and quicker program. Similar to the MASS model, WindMap is a mass-conserving wind flow model. Depending on the size and complexity of the region it can improve the spatial resolution of the MASS simulations to account for the local effects of terrain and surface roughness variations. The main meteorological data input into the models came from

reanalysis data, rawinsonde data, and land surface measurements. The reanalysis database is a gridded historical weather dataset produced by the US National Centers for Environmental Prediction (NCEP) and National Center for Atmospheric Research (NCAR). The data input into the models establish the initial conditions and updated lateral boundary conditions for the MASS model. The resolution of the MASS model could be as small as 100 to 400 m. This is dependant on the availability of the necessary topographical and land cover data. For Missouri, the main geophysical contributors are elevation, land cover, vegetation greenness (normalized differential vegetation index, or NDVI) and soil moisture (Brower, 2005). The roughness of the surface was also taken into consideration through the WindMap program. Table 3.1 shows the roughness length values that were assumed in creating the Arc GIS wind map.

Description	Roughness (m)
Perennial Snow and Ice	0.003
Cropland	0.03
Grasslands/ Herbaceous	0.05
Shrubland	0.07
Deciduous Forest	0.9
Evergreen and Mixed Forest	1.125
Wetland	0.66
Residential and Urban	0.3

Table 3.1 Provides the roughness length for the dominant land cover types (Brower, 2005).

The wind map was created using several steps. In the first step 366 days are chosen from a 15 year period through a randomized sampling scheme to equally represent each month and season in the sample. The MASS model then simulates weather conditions for the 366 days selected. Each simulation provides weather variables including wind, temperature, pressure, moisture, turbulent kinetic energy and heat flux in three dimensions throughout the model domain. The information is stored hourly. When the MASS runs are complete, summary data files are assembled from the results. The files are then input into the WindMap program for the final mapping stage which generates two main products. Firstly, color coded maps of mean wind speed and power density are created for various heights above the ground. Secondly, data files containing wind speed and direction frequency distribution parameters are output. The maps and data are then compared with land and ocean surface wind measurements as a form of quality control. If significant inconsistencies are found, the wind maps can be changed accordingly (Brower, 2005).

The sources of error affecting the accuracy of MesoMap are noted to be the finite grid scale of the simulations, errors in assumed surface properties such as roughness and errors in the topographical and land cover data bases. The finite grid scale of the simulations smoothes terrain features such as mountains and valleys. This can create inaccuracies in the wind speed data by overestimating wind speed in areas where mountains block the flow, and underestimating wind speed in areas where the flow is forced over the terrain.

“Errors in the land cover data are more common, usually as a result of the misclassification of aerial or satellite imagery. It has been estimated that the global 1 km land cover database used in the MASS simulations is 70% accurate,” (Brower, 2005). Land use is also susceptible to change with time due to urbanization, deforestation, changes in crop type or the grazing of farmland. The roughness value assigned to the terrain can also be questionable. The roughness of the surface changes through the year as seasons change and crop growth reduces or heightens. Since there are many different types of forests it is difficult to assign one value for their roughness characteristics, especially when deciduous trees are present. Forests may include many different varieties of trees with different types being predominant. To account for all different types with a single roughness value is impossible and can only be resolved by acquiring more information about the area, but this is unrealistic on a large scale. Thus, the maps are thought to be accurate in representing the overall wind energy resource, but estimates at any site should be validated by actual observational measurements.

3.2 Tall Tower Data

All the observational data from this study was collected during the period of July 2006 to March 2007. The data time period varies from tower to tower based on when the tower was equipped. Six tall towers were used in this study along with one wind profiler. The wind profiler data was obtained from July 2006

to March 2007 to encompass all of the tower data. The following sections describe tower selection processes, tower set-up, analysis of the tower data and analysis of the wind profiler data in conjunction with the tower data.

3.2.1 Tower Selection

The locations of the towers were determined using several criteria. First, the wind map was used to establish areas of strong winds. The map displays average wind speeds across the State of Missouri at heights of 30, 50, 70 and 100 m above ground level. This map is displayed in Figure 3.1 for the 100 m wind speed level. After locating the areas of strong winds using the wind map, corresponding towers were found as potential towers for the study. All the towers used in this study were pre-existing towers with heights between 100-150 m. The tall tower owners were then contacted for permission to place our equipment on their towers. This narrowed down the number of potential candidates as some owners were reluctant to allow us access to their towers. We settled on the following tower locations due to availability and location: Blanchard, Chillicothe, Maryville, Miami, Mound City and Raytown. All of the towers used in this study are located in the Northwestern portion of Missouri as the strongest winds in the state are located in this area.

Tower location	FCC #	Latitude	Longitude	Site Elevation (M)	Tower Height (M)	Overall height above MSL (M)
Blanchard	1003309	40-33-34.0	95-13-28.0	328	155	483
Maryville	1002208	40-21-36	94-53-01	353	151	505
Mound City	1007070	40-04-11.0	95-11-41.0	340	126	466
Miami	1029923	39-16-49	93-13-44	236	122	358
Chillicothe	1002160	39-48-48	93-35-26	244	152	396
Raytown	1230974	39-02-29	94-29-19.8	265	152	417

Table 3.2. Tower Information including latitude, longitude, the elevation at the site, the tower height and the total height above mean sea level are provided. The latitude and longitude are given in degrees, minutes, seconds.

While figure 3.1 displays the tower locations overlaid on a map of the mean wind speeds found at 100 m. It is also shown that the towers are well distributed, but also concentrated in Northwestern Missouri. Figure 3.2 provides a view of the Miami tower and the equipment installed on the tower.

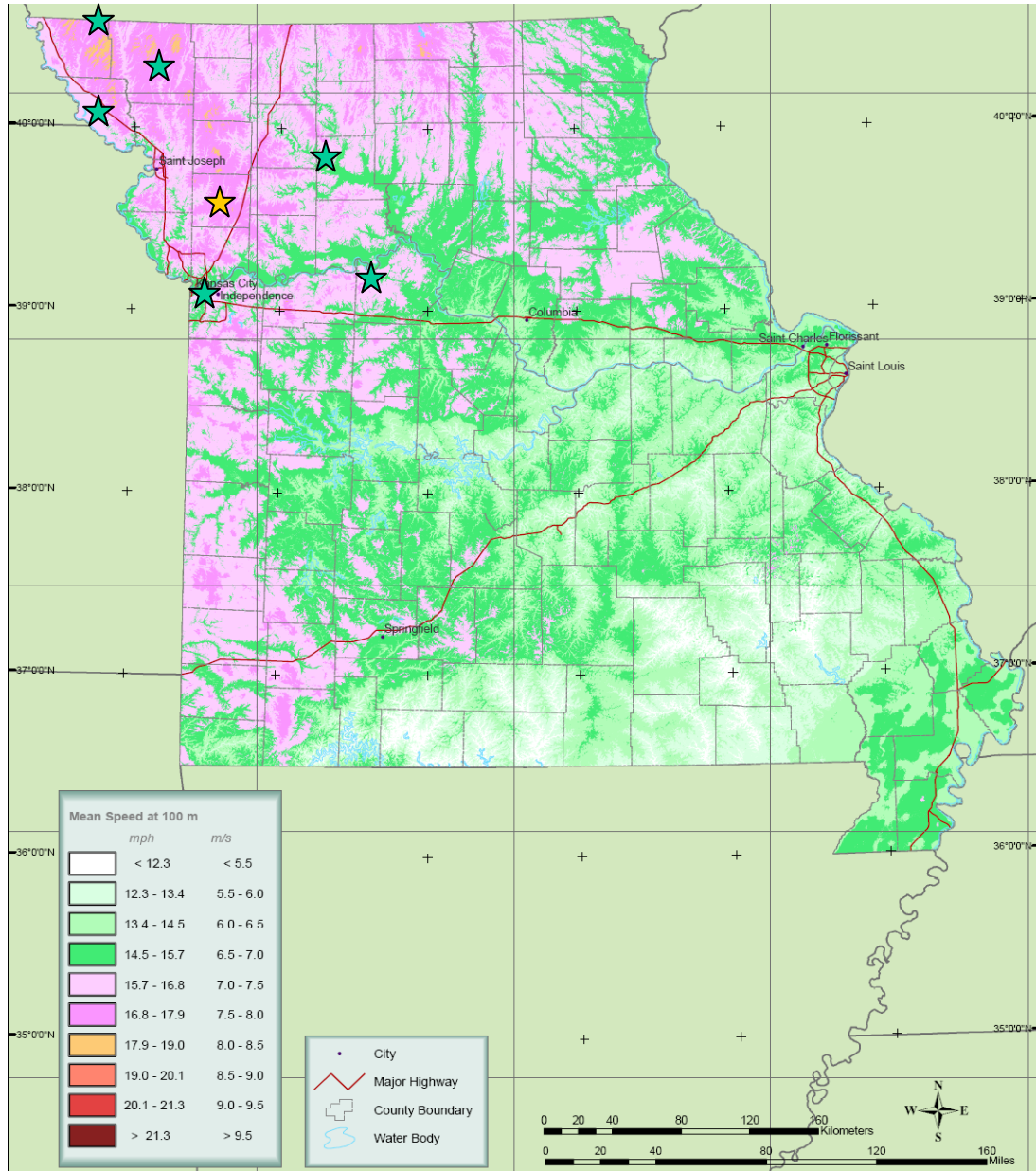


Figure 3.1. The green stars indicate the locations of the tall towers equipped, while the yellow star represents the location of the wind profiler the tower data was compared with (AWS Truewind, 2005).



Figure 3.2. An image of the Miami tower. The equipment installed can be clearly distinguished at the three heights on the tower.

3.2.2 Tower Set-up

The goal was to get instruments up on towers at the height at which wind turbines operate. Therefore, we put up two anemometers and one wind vane at heights of 70m, 100m, and then somewhere above 100m. More specifically, each anemometer was mounted on a boom 113" long and weighing 17.3 lbs. Each set of two booms was placed at 180° to one another, either on the north and south sides of the tower or northwest and southwest sides. This configuration was chosen to reduce the error that occurs with anemometers involving the effects of the tower, boom and other mounting arrangements on the

wind flow. Since there were three instruments at each height three cables needed to be run down the tower from each height to a logger mounted at ground level. The data gathered from the towers was originally intended to be accessed through a cell phone connection which would deposit the data into an e-mail account. This process was employed with the Chillicothe and Raytown towers, but could not be carried out on the remaining four towers for various reasons. Thus the data from the remaining four towers was collected manually. These instruments were meant to be in place for a period of 18 months with the option to keep them up longer if it would be beneficial to the project. Various licensed tower maintenance groups were employed to conduct the above-mentioned work.

3.2.3 Instrumentation Specifications

The NRG #200P wind direction vane was the chosen instrument for measuring wind direction in this study. It is the industry standard wind vane and its specific use is aimed towards wind resource assessment and meteorological studies. The wind vane operation can be explained by its being directly connected to a conductive plastic potentiometer located in the main body of the instrument. The potentiometer linearity accuracy is within 1%. An analog voltage output directly proportional to the wind direction is then produced when a constant DC excitation voltage is applied to the potentiometer. Measurements are taken for a scope of 360° as would be expected for a wind vane. The

threshold response characteristic is 1 m/s and the instrument operates for a range of temperatures between -55° C to 60° C. The wind vane is said to operate in 0-100% humidity conditions as well. A picture of the wind vane is provided in Figure 3.3.



Figure 3.3. An image of the wind vane equipped on each observational tower provided by the NRG Systems Specifications Report.

The NRG #40 anemometer is the industry standard anemometer and was the anemometer employed in our study. NRG #40 anemometers have been known to record wind speeds of 96 m/s. The low moment of inertia, provided as $68 \times 10^{-6} \text{ S-ft}^2$, and unique bearings allow for a very rapid response to gusts and lulls. Because of their output linearity, these sensors are ideal for use with an assortment of data retrieval systems including NRG Software which was utilized in this study. The anemometer operates using a four pole magnet which induces a sine wave voltage into a coil producing an output signal with a frequency proportional to the wind speed. The accuracy of the instrument is within 0.1 m/s

for the range of 5 m/s to 25 m/s wind speeds. The operating temperature of the anemometer is -55°C to 60°C and it operates in 0-100% relative humidity. Figure 3.4 provides an image of the type of anemometer equipped on each observational tower.



Figure 3.4. An image of the anemometer placed on each observational tower provided by the NRG Systems Specifications Report.

3.2.4 Analysis of Tower Data

The tower data utilized in this study consists of nine channels worth of data. The first two channels represent the anemometer readings from the lowest level on the tower, generally near 70 m. Channels 3 and 4 record data from the anemometers placed near 100 m. Channels 5 and 6 then record the data from the anemometers placed highest on the tower, above 100 m. The wind vanes for each level are represented by channels 7, 8 and 9 with channel 7 placed at the height of channels 1 and 2, channel 8 at the same height as channel 3 and 4 and

channel 9 at the same height as channels 5 and 6. Data collection began for the Miami tower in July 2006, but for most towers the dataset begins in August 2006. The length of the dataset is dependent on when the tower was equipped with the wind vanes and anemometers. Table 3.2 illustrates the dates each tower was set-up as well as the heights of each instrument.

Tower Site	Date Equipped	CH 1 Height (m)	CH 2 Height (m)	CH 3 Height (m)	CH 4 Height (m)	CH 5 Height (m)	CH 6 Height (m)
Blanchard	8/4/2006	61	61	97	97	137	137
Chillicothe	10/4/2006	61	61	97	97	137	137
Maryville	8/3/2006	61	61	97	97	117	117
Miami	7/2/2006	67	68	96	97	114	115
Mound City	8/6/2006	61	61	97	97	117	117
Raytown	8/4/2006	67	67	95	95	140	140

Table 3.3. Displays the date each tower was equipped with the instruments as well as the heights of the instruments on each channel.

Quality control was performed manually on the data to remove the erroneous wind speeds recorded by the instruments on the tower. At times when the equipment was not working properly, work was being done on the tower or data was being collected from the instruments a value of 0.4 was recorded. Thus these values needed to be replaced with NaN (not a number) so as to not distort or misrepresent the data when correlations were performed. A value of 0.4 was also recorded in times of icing. Since data was collected during the winter months, icing was a major issue. There were several periods during which the wind vanes and anemometers were frozen and unable to record data. Even after the instruments had thawed the effects of the ice could still be seen through low or calm wind speeds. Thus the periods where ice prevailed needed to be

removed from the dataset. Once this was completed we could proceed with the analysis using our clean dataset.

The data retrieved from the six towers was analyzed using Matlab and Microsoft Excel. Microsoft Excel was used to determine the average monthly wind speed for each channel. These averages were used to create one average wind speed for each tower location over the period that the towers were recording data. Each tower's average was then compared to the corresponding wind speed taken from the Arc GIS wind map created by AWS Truewind Ltd.- commissioned by Missouri DNR to see how well the speeds match up. The wind speeds from the towers were compared to the wind maps in a general fashion to determine if the wind maps are a good representation of Missouri's wind resources.

The data was also imported into Matlab where we formed routines to organize and analyze the data necessary to the objectives. Matlab was utilized to create diurnal variation plots to confirm the presence of a pattern within our data. These plots were made for each month at each tower for each of the six channels. All six channels were plotted on the same graph to best view the diurnal variation. Graphs of tower winds versus profiler winds at 500 m above sea level were also made for each month at each tower for each of the six channels to determine if a correlation was present.

Wind speed versus time plots were created for each month at each tower for just the 6th channel. These plots showed the variation in wind speed throughout the entire month for the 6th channel. Plots were also made to determine if there

is a threshold for locating low-level jet occurrences. To determine this, winds from the tower site were extrapolated to 500 m and plotted against the 500 m profiler winds to determine if a correlation was present. Lines of one standard deviation were added to these plots to determine where the majority of the outliers were located. The location of the low-level jet is thought to be related to the location of the outlying points and this will be further described in Chapter 4.

3.3 Wind Profiler

Wind Profiler data was collected from <http://mtarchive.geol.iastate.edu> for Lathrop, MO to be compared with the observational tower data. The latitude of the wind profiler is 39-34-48W and the longitude is 94-11-24N. The Lathrop, MO profiler was chosen because it is the only profiler in the northwest portion of Missouri. The profiler also happens to be conveniently situated among the center of the tower locations. The Lathrop, MO wind profiler is a part of the NOAA profiler network. Thus, the winds provided at each height are averaged hourly from 6 minute measurements taken from the preceding hour of data (NOAA). The observational tower data was also an hourly average, but made using 10 minute measurements. The displayed profiler winds have all "passed" single-station quality control (continuity) requirements and typically represent high quality data (NOAA). Table 3.4 provides the distance of each tower from the profiler and the direction of the tower in regard to the wind profiler.

Tower	Direction from Profiler	Distance from Profiler (km)
Blanchard	NW	140
Chillicothe	ENE	57
Maryville	NNW	105
Miami	SE	89
Mound City	NW	101
Raytown	SSW	65

Table 3.4. The direction of each tower is provided with regard to the wind profiler in Lathrop, MO and distance of each tower from the profiler is also given.

3.3.1 Analysis of Wind Profiler Data

The wind profiler data was obtained from the Mtarchive Data Server. This server archives the wind profiler data in a gempak format. Therefore, the data had to be converted from gempak to ASCII format to be usable in Matlab. Thus a FORTRAN program was assembled to retrieve the data and then convert the data to a more user-friendly format. An additional round of quality control was performed manually on the dataset to ensure its reliability. The profiler data was then fed into Matlab where it was used to create the graphs of tower winds versus profiler winds at 500 m above sea level. The profiler winds were correlated to the surface winds to determine if the upper-level profiler winds could be extrapolated to the surface and used as an estimate for the surface winds. The profiler winds also assisted in determining a threshold for the location of the low-level jet. In this case the tower winds were extrapolated upwards to 500 m

and correlated to the profiler winds. Lines were added to the chart denoting plus/minus one standard deviation. The logic was to determine the location of the low-level jet depending on where the most outliers were found. As part of this investigation terrain following coordinates were tested against pressure following coordinates to determine if a noticeable difference was present. Terrain following coordinates are those that simply measure above ground level or the surface. Using pressure coordinates each tower is placed at mean sea level so that they are on a level ground. Since we are measuring winds that will be affected by the surface characteristics it is probably best to use terrain following coordinates. Also, the low-level jet has been found to follow the local terrain (see Pichugina et al., 2004, for example) providing further reason to utilize the terrain following coordinates as opposed to pressure coordinates. However, only a negligible difference was detected in correlations when comparing the two coordinate systems.

Chapter 4 Results and Discussion

4.1 Results

The following section will be a presentation of the results obtained through this project. A discussion of our theories will also be provided.

4.1.1 Verification of Current Wind Maps

To verify the current wind maps a simple yet effective comparison was produced. First, we obtained wind speed estimates from the wind map by locating our tower sites using the latitudes and longitudes provided in Table 3.2. The wind speeds were recorded for the 50, 70 and 100 m heights as shown in Table 4.1.

Tower Location and Rank	50 m wind speed (m/s)	70 m wind speed (m/s)	100 m wind speed (m/s)
Blanchard (1)	6.79	7.32	7.92
Maryville (2)	6.70	7.31	7.99
Mound City (3)	6.46	6.99	7.62
Miami (4)	6.33	6.82	7.37
Chillicothe (5)	5.95	6.51	7.17
Raytown (6)	5.63	6.25	6.95

Table 4.1. Displays the 50, 70, and 100 m annual mean wind speeds provided by the wind map.

Towers were also ranked according to which had the greatest wind speed with a ranking of '1' given to the tower with the strongest winds. These rankings were compared to rankings compiled using the observational tower data. The observational tower measurements are located in Table 4.2. Table 4.2 provides the average wind speed recorded for each channel on each tower during the months of operation. When figuring the average wind speed for the ranking all tower data was included except that which contained error. So, the data from times of icing or other instances that incurred erroneous data were excluded.

Tower Location and Rank	Ch1 wind speed (m/s)	Ch2 wind speed (m/s)	Ch3 wind speed (m/s)	Ch4 wind speed (m/s)	Ch5 wind speed (m/s)	Ch6 wind speed (m/s)
Blanchard (1)	NA	6.81	NA	7.69	NA	8.11
Maryville (2)	6.61	6.41	7.31	7.48	7.71	7.8
Mound City (5)	5.64	5.82	6.37	6.24	6.80	6.93
Miami (3)	6.14	5.97	6.1	6.63	7.12	7.41
Chillicothe (4)	6.06	5.89	6.59	6.61	7.43	7.33
Raytown (6)	4.99	5.11	5.92	5.95	6.79	7.28

Table 4.2. Displays each channel's average wind speed throughout the months of operation.

The rankings from the wind map and the observational network were then compared generally to determine if a correlation was present. The third and fourth channels were chosen to make this comparison because they are located just below 100 m for each tower and a wind speed is produced for 100 m by the wind map. The fifth and sixth channels could not be used because they are located at different heights for each tower and are unable to be compared among the towers. The two sets of data were only generally compared because a year's worth of observational data was not present for the towers. The wind speeds

taken from the wind map include seasonal variations while the observational data only covers eight months of the year for most of the towers with the exception of nine months of data for the Miami tower and only six months for the Chillicothe tower. Thus, the data would not be expected to match the estimates given by the wind map because it is not extensive enough. Once a year of data is available from the observational network, a better correlation can be made.

The period of record for each tower does vary depending on when the instruments were installed. This variation in the dataset was accounted for in comparing the observed wind speeds to the wind map and in ranking the observed wind speeds among each other. Table 4.2 does display the average wind speed for the entire period of operation for each tower. Since all the towers were operational for the period of October to March an average was also made for that time. In averaging the wind speeds from October to March the ranking is found to be the same as that determined by the overall average for the sites. Thus, the ranking still matches the wind map in the same fashion. It may also be noticed that the observed wind speeds for the channels located at the same height on the same tower vary. These variations are most likely caused by tower interference since each anemometer is placed at a different angle from the tower. As a result, one anemometer may record stronger winds than the other since it is not blocked by the tower. These differences may also be attributed to times of icing. When the instruments freeze and stop recording data because of freezing rain or ice, it takes them different amounts of time to become active again which interferes with data collection.

Through our rough correlation we did find that the wind map and tower data match up well when the rank of each site is compared. The only discrepancy occurs with the Mound City site. It drops in rank from the third windiest site to the fifth. Once a year of data is available it will be interesting to compare the wind map to the observational findings.

At this time, we are noticing that the observational wind speeds are a bit lower than those estimated by the wind map. If this trend is still present once a year of observational data is available, it may suggest that the wind map is overestimating the wind resource in Northwestern Missouri. These differences may be due to the roughness parameter used in the modeling of the wind map. Since the wind map only distinguishes among eight types of land cover, two of which are not present in Missouri, the roughness parameter may not be representative of the area it is assigned to. Differences in the wind speeds could also be attributed to the fact that climate data has been utilized in creating the wind map whereas even a year of data is not enough to fully account for wind speeds in an area. Longer periods of observational data collection would be beneficial and provide a more reliable verification of the wind map. The wind map is also estimating wind speeds for 100-m heights, whereas the towers are measuring the wind speed a few meters below this height which may be responsible for the difference. In conclusion, the wind maps were roughly verified by the observational data which is a very important first step in siting areas for wind resource development.

4.1.2 Diurnal Variation

The most important aspect when considering a site is the windiness. Since most wind turbines begin operation at a speed of 4-5 m/s and reach maximum power at about 15 m/s, it is critical to have a site that can produce wind speeds within this range. The power available from the wind is a function of the cube of the wind speed. Therefore a doubling of the wind speed gives eight times the power output from the turbine. All other things being equal, a turbine at a site with an average wind speed of 5 m/s will produce nearly twice as much power as a turbine at a location where the wind speed averages 4 m/s (BWEA, 2006). This makes it very important to determine the average wind speed, but also the time maximum wind speeds will occur so that the turbines are in operation during that period.

One way to determine the period of maximum wind speeds is to examine the diurnal variations for a particular site. Seasonal variations within the diurnal pattern should also be observed to identify the time of year to expect the strongest winds. Utilizing the observational tower data we have constructed diurnal variation plots using monthly data, so we have created a plot for each tower site, for each month. The only data excluded in compiling the diurnal variation plots is missing data and the data that had incurred error. Figures 4.1 through 4.5 show the diurnal variation plots prepared for each tower.

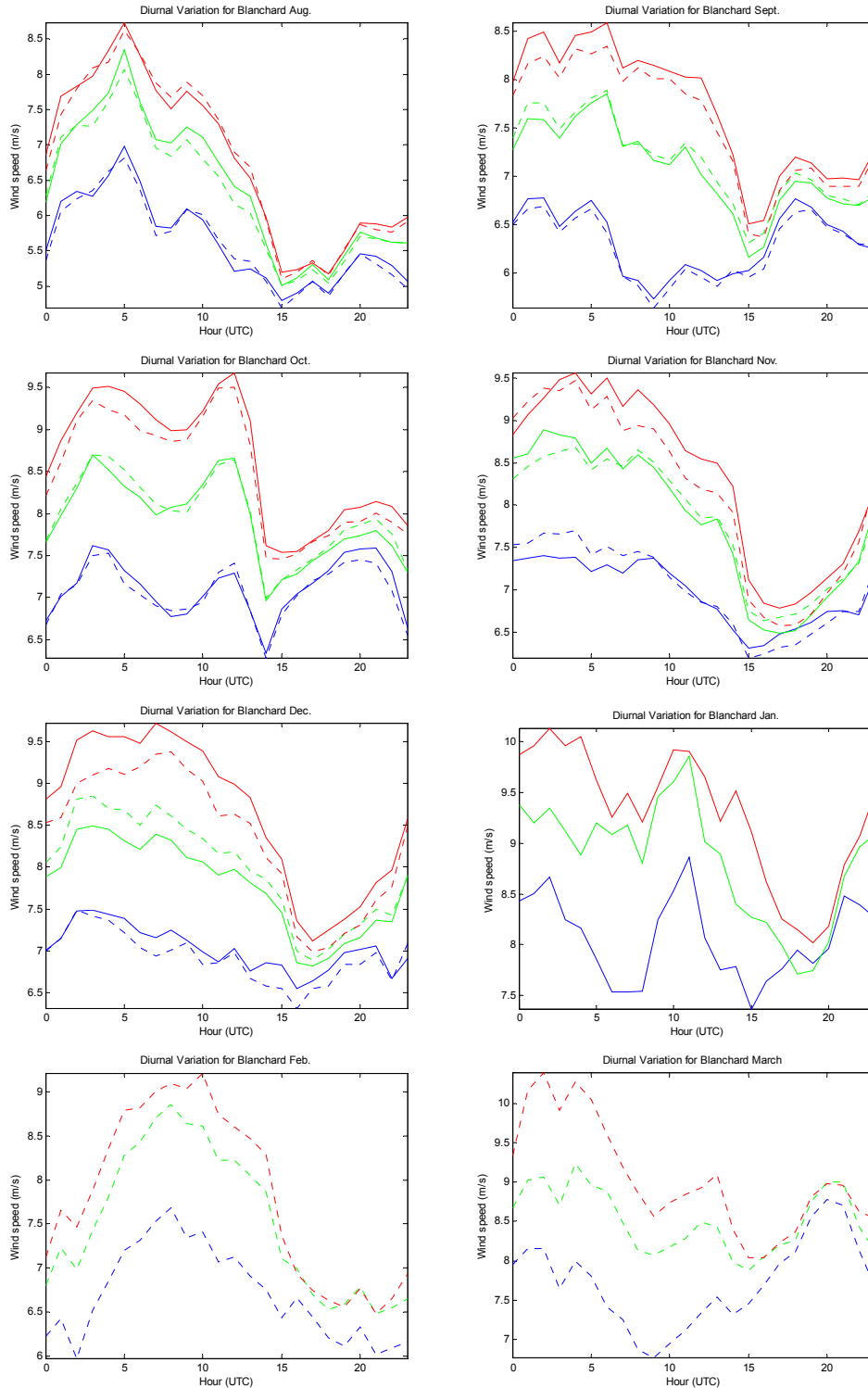


Figure 4.1. Diurnal variation plots for the Blanchard Tower. The blue solid line represents Channel 1, the blue dashed line is Channel 2, the green solid line is Channel 3, the green dashed line is Channel 4, the red solid line is Channel 5 and the red dashed line is Channel 6.

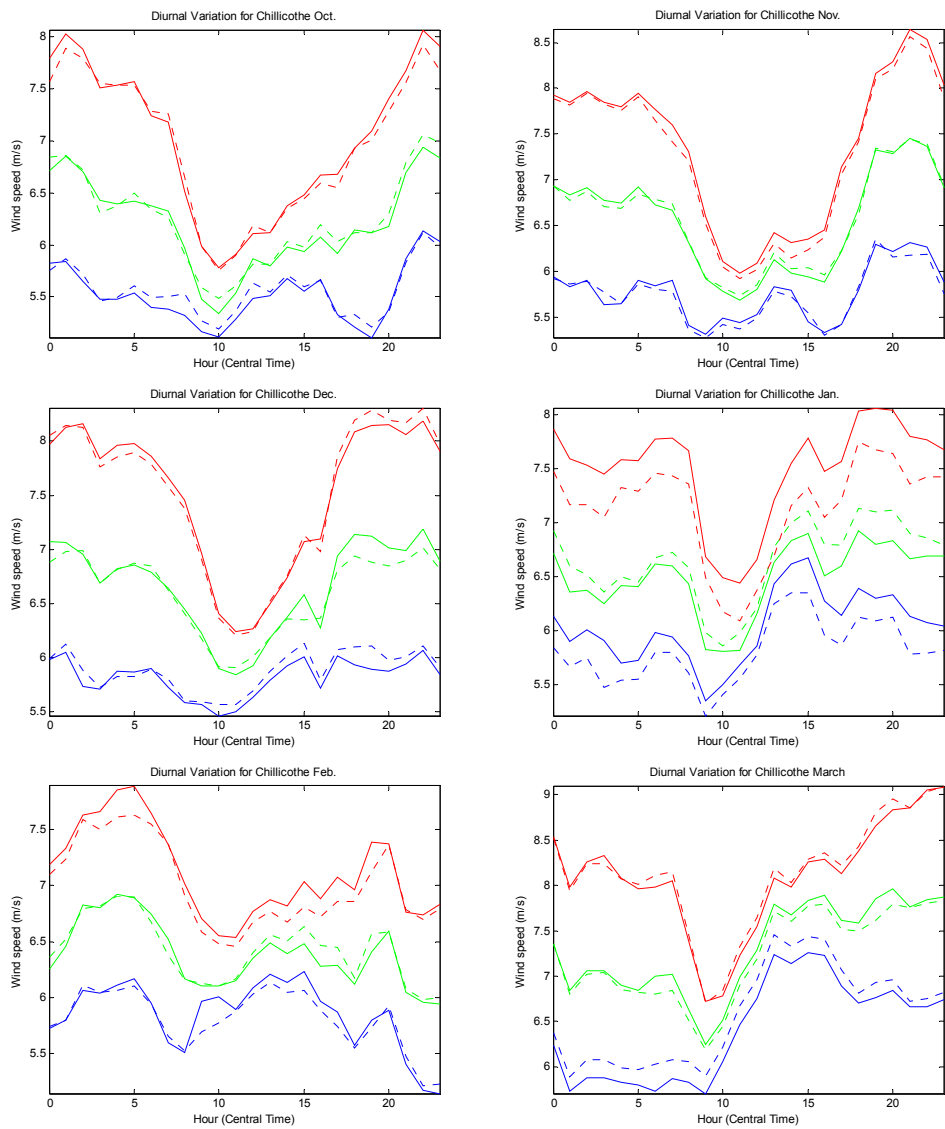


Figure 4.2. Diurnal variation plots for the Chillicothe tower. The blue solid line represents Channel 1, the blue dashed line is Channel 2, the green solid line is Channel 3, the green dashed line is Channel 4, the red solid line is Channel 5 and the red dashed line is Channel 6.

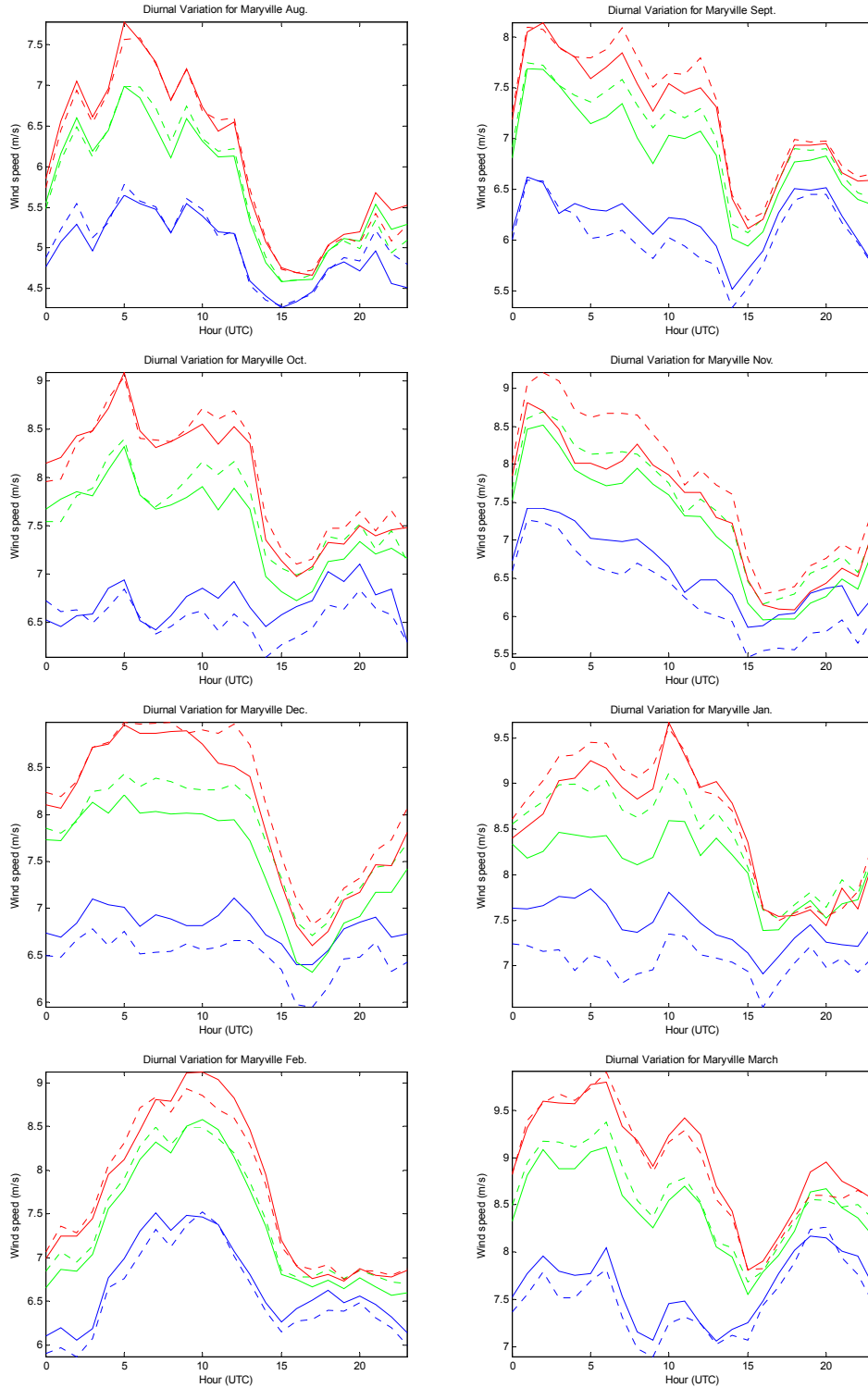
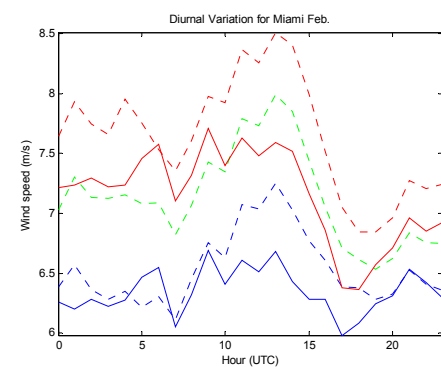
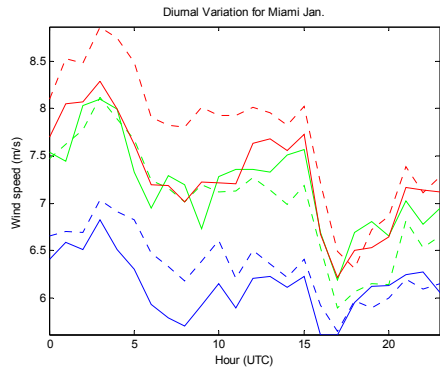
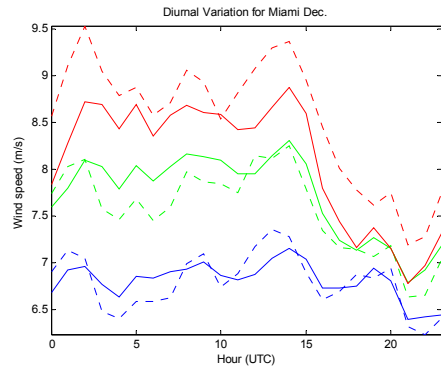
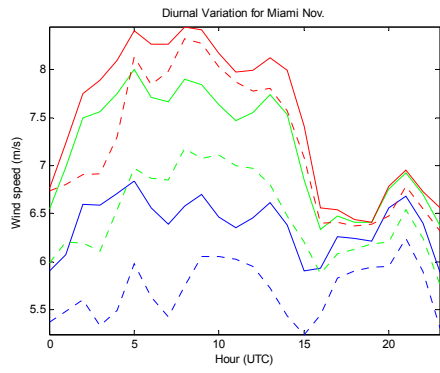
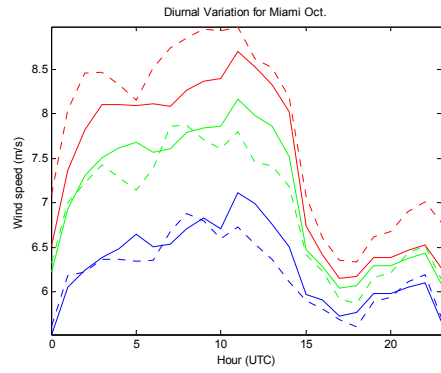
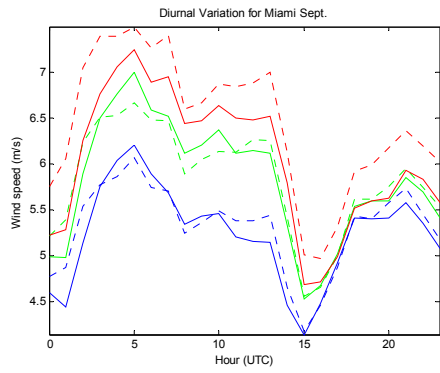
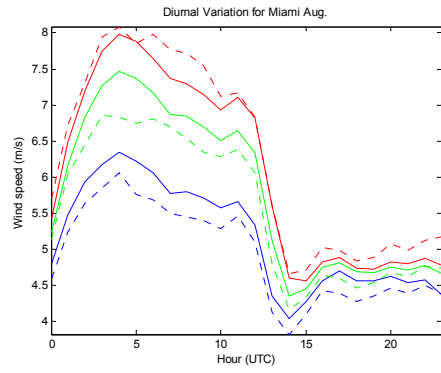
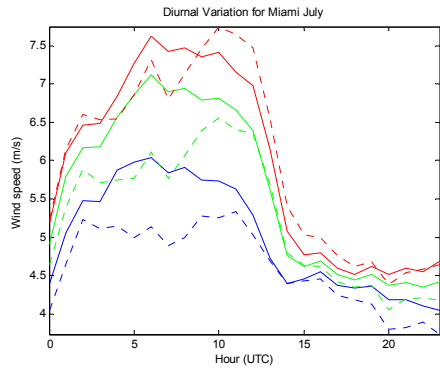


Figure 4.3. Diurnal variation plots for the Maryville tower. The blue solid line represents Channel 1, the blue dashed line is Channel 2, the green solid line is Channel 3, the green dashed line is Channel 4, the red solid line is Channel 5 and the red dashed line is Channel 6.



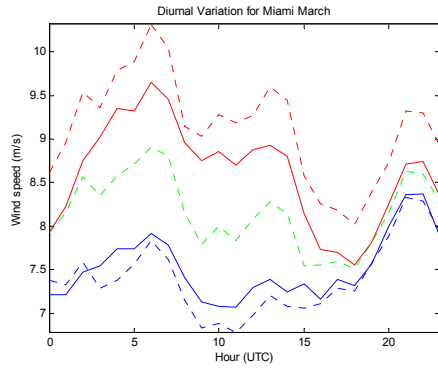


Figure 4.4. Diurnal variation plots for the Miami tower. The blue solid line represents Channel 1, the blue dashed line is Channel 2, the green solid line is Channel 3, the green dashed line is Channel 4, the red solid line is Channel 5 and the red dashed line is Channel 6.

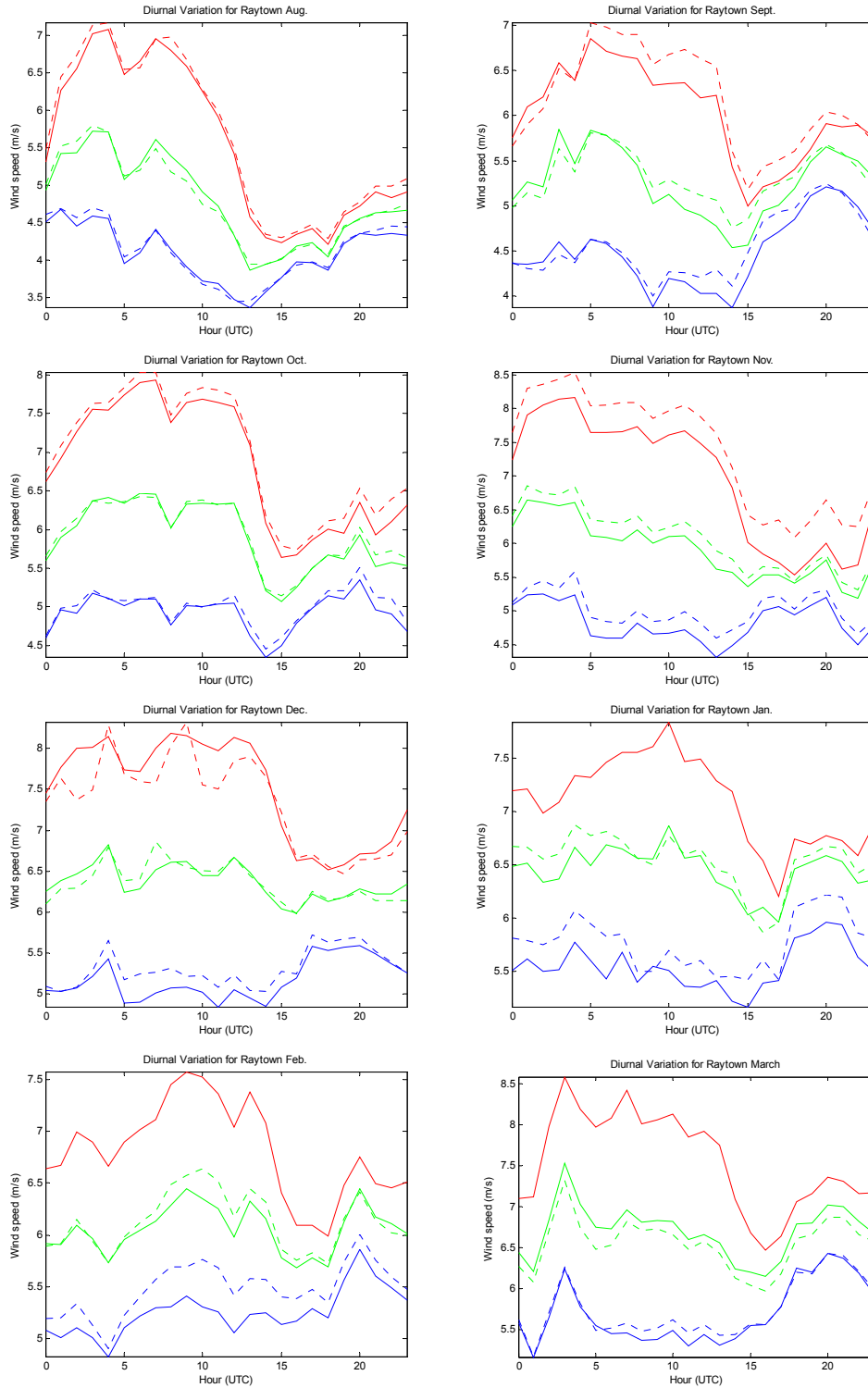


Figure 4.5. Diurnal variation plots for the Raytown tower. The blue solid line represents Channel 1, the blue dashed line is Channel 2, the green solid line is Channel 3, the green dashed line is Channel 4, the red solid line is Channel 5 and the red dashed line is Channel 6.

Some interesting effects shown by the diurnal variations include seasonal changes. It can be seen for each tower that the wind speed increases throughout the winter and early spring months. This finding indicates that the best time to harness wind energy resources would be from October to at least March. The spring months following March may have strong winds as well, but since the observational dataset ends in March we are unable to make conclusions based on data that has not yet been examined. Another commonality among the diurnal variations is the dip that takes place as a result of the lack of solar radiation during the evening hours. At the levels measured by our towers this wave is approximately 180° out of phase with the surface as can be seen in Figure 2.1. This dip is seen at approximately the same time for each tower, regardless of month.

To determine when the strongest winds will occur, we can also look to charts of wind speed versus time for each month. Figure 4.6 through 4.8 provide such charts for the Maryville tower for the months of August, November and February. The Maryville tower was chosen because it is a good representation of how the wind speeds from the wind profiler correspond to the observed wind speeds from the tower. Really, any of the tower sites could have been chosen because they all correspond well with the profiler for each month. The months of August, November and February were chosen to show that the relationship is present throughout our period of data collection. In the charts of wind speed versus time the hourly data is presented for an entire month, as opposed to the average of a month's worth of data for the diurnal variation plots provided earlier.

Once again, the only data not included in these plots is the data where error was incurred. In showing the hourly data for an entire month it is possible to view the fluctuation that naturally occurs as well as the maximum and minimum wind speeds. It can be seen in Figures 4.6 through 4.8 that the observed winds do not always pick up on the more pronounced peaks. This suggests that the LLJ is not always transferred to the surface. In these cases the LLJ is most likely located completely above the 100-m height where the tower wind speeds are measured, but in the vicinity of the 500-m height of the wind profiler.

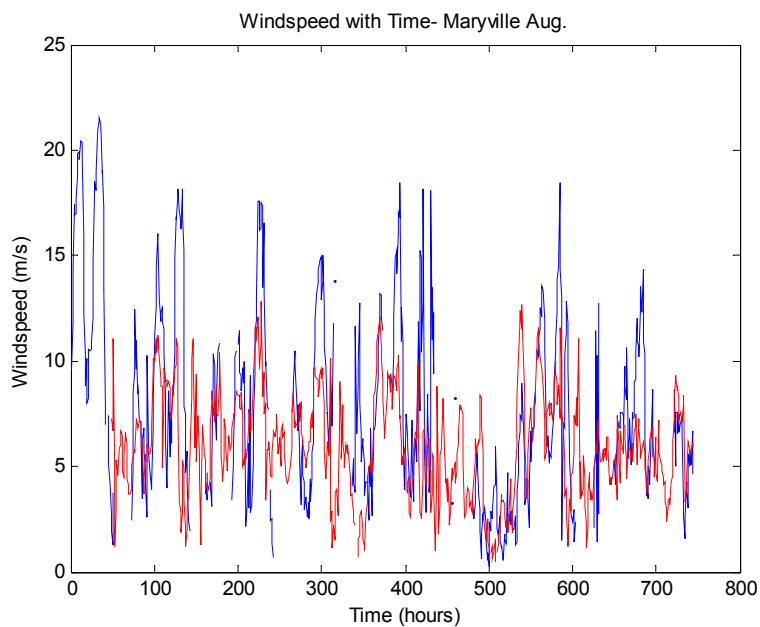


Figure 4.6. The variation of wind speed with time for the month of August, 2006 at the Maryville site. The wind profiler wind speed measurements are shown in blue and the observed tower winds for channel 6 are shown in red.

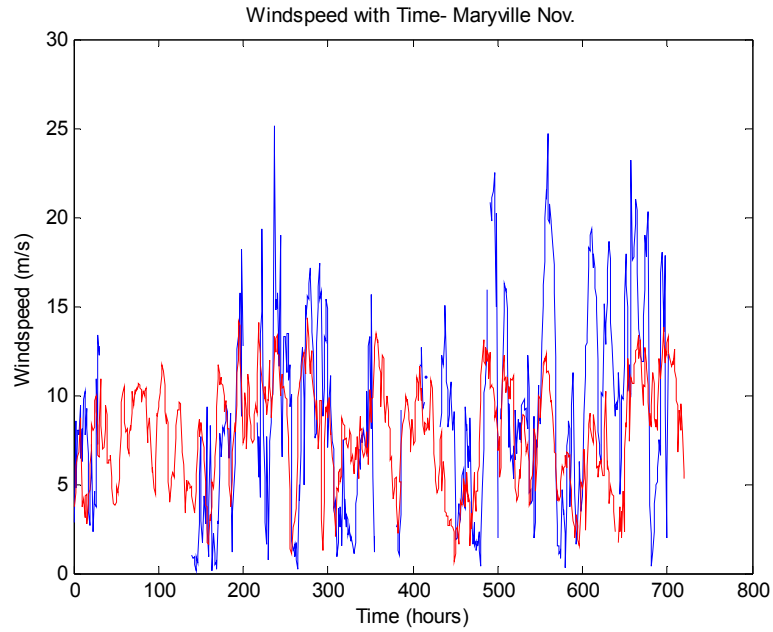


Figure 4.7. The variation of wind speed with time for the month of November, 2006 at the Maryville site. The wind profiler wind speed measurements are shown in blue and the observed tower winds for channel 6 are shown in red.

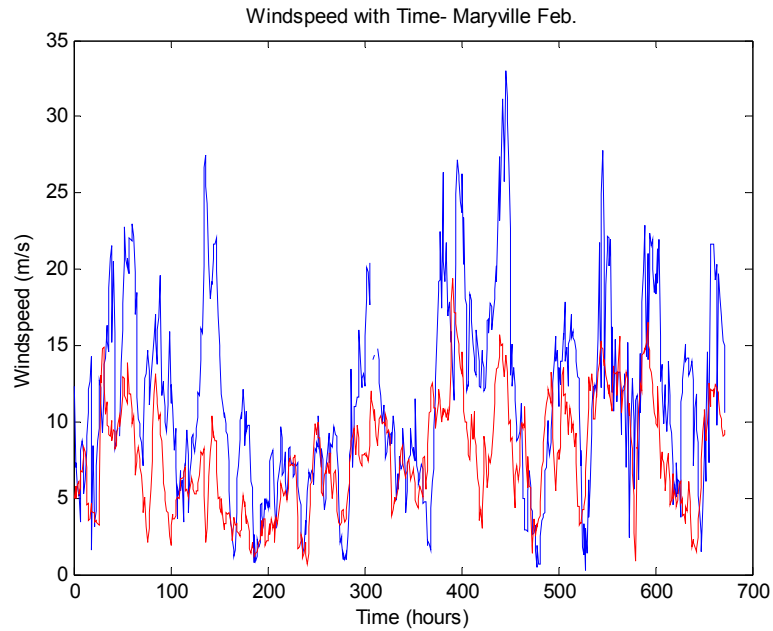


Figure 4.8. The variation of wind speed with time for the month of February, 2007 at the Maryville site. The wind profiler wind speed measurements are shown in blue and the observed tower winds for channel 6 are shown in red.

When the observed diurnal variation plots are compared with the expected cycle, shown in Figure 2.1, it can be seen that the two match up well. This finding is important because it validates the observed data. The relationship between the tower data and wind profiler data further validates the data collected from the tower sites. Had the observational data not corresponded to the expected pattern, our dataset may be prone to large errors and may not be usable for more in-depth research applications.

4.1.3 The Use of Profiler Winds as a Proxy for Surface Winds

Normally, surface data is extrapolated upward through the boundary layer to produce estimates of upper-level winds. Since this method is prone to errors, we wanted to test and see if the reverse of this theory may provide a reasonable estimate for surface wind speeds. So, data collected from the observational network of towers was compared with profiler winds to determine if profiler winds can be used as a proxy for surface winds. The profiler wind speed at 500 m was plotted against the third and fourth channels to determine if a correlation was present. The third and fourth channels were chosen because they are located at the same height for each tower so we are able to compare findings among the different tower sites. We also have data available from the wind map for these heights. In constructing these plots the only data emitted was that which had incurred error through icing or other circumstances. A few of these plots are shown in Figures 4.9 through 4.13 to demonstrate how the comparison was

carried out. The line plotted on each chart is a polynomial fit. A polynomial fit finds the coefficients of a polynomial $p(x)$ of degree n that fits the data in a least squared sense. The line is then given by the equation:

$$p(x) = p_1x^n + p_2x^{n-1} + \dots + p_nx + p_{n+1} \quad (4.1)$$

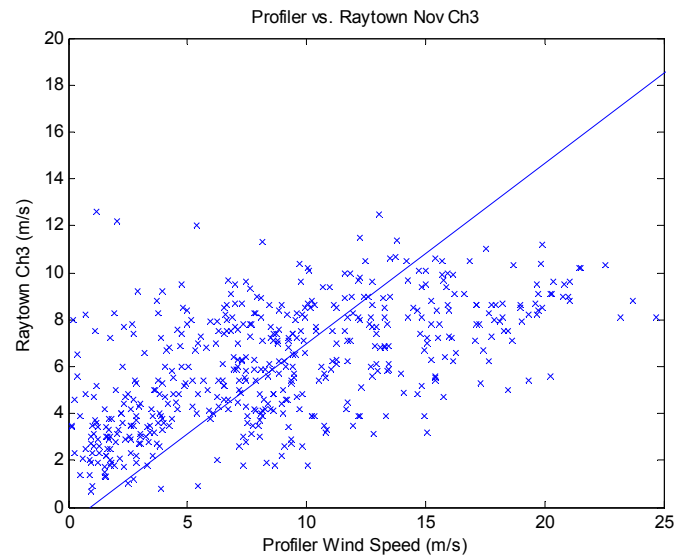


Figure 4.9. The wind profiler wind speed at 500 m is plotted against the wind speed from channel 3 of the Raytown tower, both for the month of November. The line plotted is a polyfit.

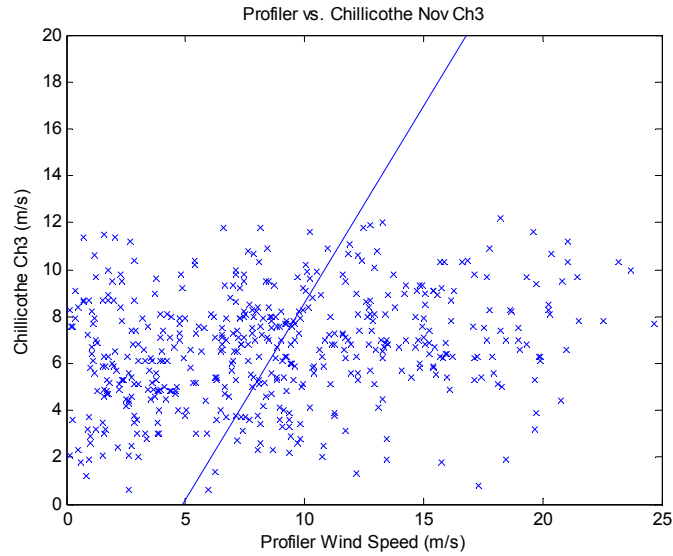


Figure 4.10. The wind profiler wind speed is plotted against the wind speed from channel 3 of the Chillicothe tower, both for the month of November.

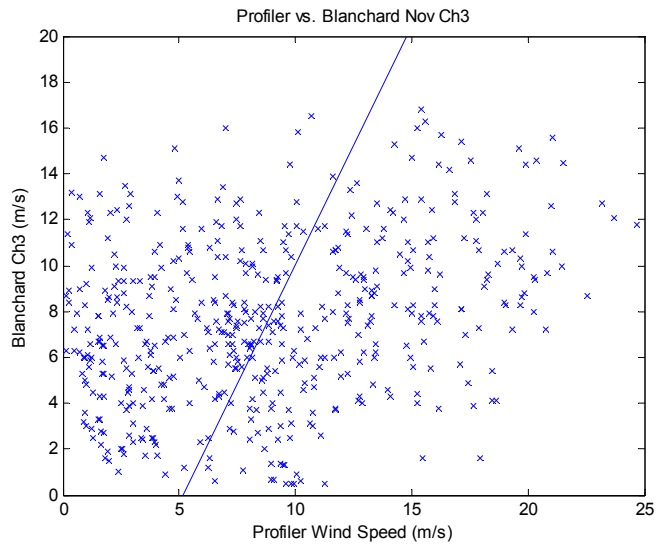


Figure 4.11. The wind profiler wind speed at 500 m is plotted against the wind speed from channel 3 of the Blanchard tower, both for the month of November.

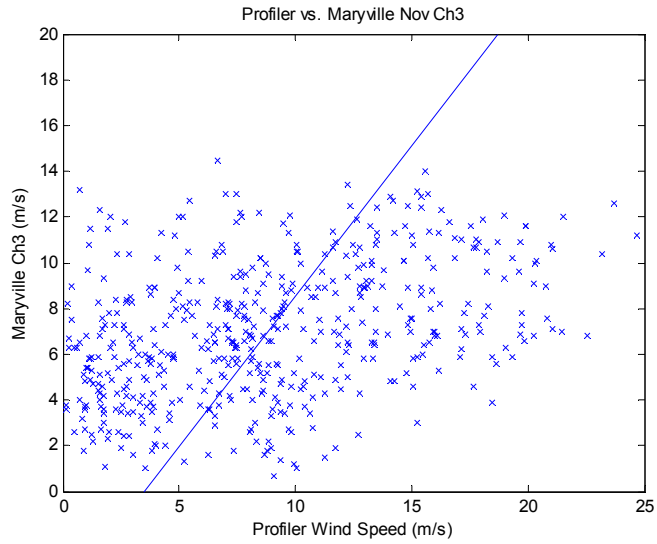


Figure 4.12. The wind profiler wind speed at 500 m is plotted against the wind speed from channel 3 of the Maryville tower, both for the month of November.

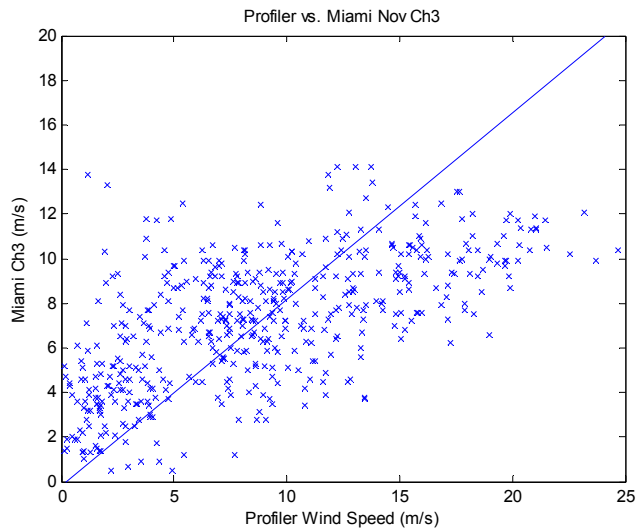


Figure 4.13. The wind profiler wind speed at 500 m is plotted against the wind speed from channel 3 of the Miami tower, both for the month of November.

Figure 4.9 is representative of a case where a better correlation was found between the profiler wind and the observed wind. The correlation coefficients obtained for each tower site are given in Tables 4.3 through 4.7. Figure 4.10 is a

situation where the correlation obtained was not as strong. It can be seen by looking at Table 4.5 that the correlation values obtained for the Chillicothe tower are consistently low compared to the other towers, especially for the month of November. The correlation coefficients for the Raytown tower are found to be stronger for each month. Even though these two towers are nearly the same distance from the wind profiler, Raytown being 65 km from the wind profiler and Chillicothe 57 km from the profiler, the correlations are quite different. This may be attributed to the direction of the tower sites relative to the wind profiler, Raytown is to the south-southwest and Chillicothe is located east-northeast of the wind profiler in Lathrop. This difference could also be attributed to the surface roughness. The surface conditions for the wind profiler and the Raytown tower may be similar with different conditions present at the Chillicothe site.

Tower Site	Blanchard							
Channel	Aug	Sept	Oct	Nov	Dec	Jan	Feb	March
1	0.3676	0.5008	0.3594	0.2718	0.4858	0.6022	NA	0.512
2	0.3720	0.5004	0.3891	0.2756	0.4894	0.4918	0.5452	0.4475
3	0.4116	0.5480	0.4234	0.2995	0.4754	0.6323	NA	0.5035
4	0.4167	0.5407	0.4194	0.3029	0.4743	0.5405	0.5469	0.4592
5	0.4442	0.5689	0.4383	0.3303	0.4693	0.6729	NA	0.5131
6	0.4358	0.5688	0.4203	0.3107	0.4582	0.5776	0.5468	0.4378

Table 4.3. Correlation Coefficients are shown for the Blanchard tower. They display the relationship between 500 m wind speeds taken from the Lathrop, MO wind profiler and the observed tower data for each channel.

Tower Site	Chillicothe					
Channel	Oct	Nov	Dec	Jan	Feb	March
1	0.3283	0.2931	0.3824	0.4759	0.4938	0.4687
2	0.3163	0.2690	0.3416	0.4413	0.4776	0.4442
3	0.3272	0.2490	0.3404	0.435	0.4601	0.4391
4	0.3407	0.2617	0.3731	0.4843	0.4764	0.469
5	0.3499	0.2515	0.368	0.4845	0.4562	0.4531
6	0.3330	0.2328	0.3284	0.4262	0.4423	0.4314

Table 4.4. Correlation Coefficients are shown for the Chillicothe tower. They display the relationship between 500 m wind speeds taken from the Lathrop, MO wind profiler and the observed tower data for each channel.

Tower Site	Maryville							
Channel	Aug	Sept	Oct	Nov	Dec	Jan	Feb	March
1	0.3808	0.5242	0.4641	0.3940	0.5138	0.5399	0.5844	0.4961
2	0.3180	0.5260	0.2347	0.3397	0.3808	0.4412	0.5512	0.4159
3	0.3724	0.5631	0.3429	0.3949	0.4082	0.5219	0.5533	0.455
4	0.4240	0.5549	0.5082	0.4292	0.5066	0.5714	0.586	0.5052
5	0.4163	0.5734	0.3758	0.3951	0.4032	0.5354	0.5662	0.4438
6	0.4441	0.5735	0.5364	0.4516	0.5177	0.5957	0.5862	0.5001

Table 4.5. Correlation Coefficients are shown for the Maryville tower. They display the relationship between 500 m wind speeds taken from the Lathrop, MO wind profiler and the observed tower data for each channel.

Tower Site	Miami								
Channel	July	Aug	Sept	Oct	Nov	Dec	Jan	Feb	March
1	0.5941	0.6228	0.5935	0.5468	0.5653	0.406	0.6735	0.5706	0.4966
2	0.4391	0.4528	0.5313	0.4319	0.3199	0.3226	0.5137	0.6835	0.4438
3	0.6272	0.6799	0.6358	0.5894	0.6135	0.4101	0.646	NA	NA
4	0.5205	0.5467	0.5516	0.5065	0.4099	0.3587	0.5312	0.6486	0.4719
5	0.6416	0.7054	0.6441	0.6147	0.6220	0.4041	0.6601	0.5688	0.5217
6	0.5672	0.5736	0.5905	0.5557	0.4627	0.3643	0.5418	0.634	0.4634

Table 4.6. Correlation Coefficients are shown for the Miami tower. They display the relationship between 500 m wind speeds taken from the Lathrop, MO wind profiler and the observed tower data for each channel.

Tower Site	Raytown							
Channel	Aug	Sept	Oct	Nov	Dec	Jan	Feb	March
1	0.5545	0.6473	0.5958	0.5965	0.5583	0.701	0.6295	0.5071
2	0.5609	0.6306	0.5874	0.6052	0.5442	0.6525	0.6303	0.4894
3	0.4831	0.6019	0.5326	0.5898	0.5612	0.7081	0.648	0.5376
4	0.5280	0.5884	0.5503	0.5746	0.575	0.6931	0.6548	0.5263
5	0.3768	0.5251	0.4509	0.5296	0.5356	0.6912	0.6538	0.5311
6	0.4165	0.5456	0.5038	0.5347	0.4256	0.7048	0.4397	NA

Table 4.7. Correlation Coefficients are shown for the Raytown tower. They display the relationship between 500 m wind speeds taken from the Lathrop, MO wind profiler and the observed tower data for each channel.

It does not appear that the correlation coefficients produced are very useful. The correlations seem to be lowest for the months of October, November and December for all of the towers. This may be related to the direction of the wind flow or the direction of the tower relative to the wind profiler. This may also be attributed to the location of the LLJ and the boundary layer. The boundary layer is generally lower in the atmosphere in the fall and winter and can be located between 100- and 500-m. In the summer the boundary layer is located higher up in the atmosphere and can be more than 1 km thick. The location of the boundary layer is important because below the boundary layer the winds are still influenced by friction with the surface and above the boundary layer the winds are more geostrophic. If the boundary layer was between the 100- and 500-m layer then it would definitely influence the correlation values obtained because the profiler wind speeds would be above the boundary in the geostrophic winds and the tower wind speeds would be located below the boundary under the influence of surface friction. So, the presence of the

boundary layer during these late fall and winter months may be responsible for these low values and could be skewing the correlation coefficients.

Based on the correlation values, the profiler winds would not be a good estimate of the surface winds. If we were to use the normal procedure of extrapolating the single height 100-m winds upward to 500 m it would not even work well in most cases. This is shown with the Chillicothe data for the month of November. In the case of the Raytown tower for the month of November, we may see a good representation of the upper-level winds when the surface winds are extrapolated upward, but some error would still be incurred. A few meters per second would make less of a difference when we are speaking of stronger upper-level winds as opposed to weaker surface winds and thus this error is more easily accepted. When extrapolating upper-level winds to the surface we must also take into account the roughness of the surface. The roughness tends to have less of an effect on wind speeds further up in the atmosphere. In extrapolating the 500 m wind speed to the surface we are unable to account for the effects of surface roughness because the 500 m winds are not as affected as the 100 m winds. Therefore, it is probably best to continue extrapolating surface winds upward in an attempt to estimate higher level winds instead of vice versa.

4.1.4 Locating the Low Level Jet

Since the low-level jet is a significant phenomenon that affects the wind speed in the Midwest, detection of the low-level jet is important. To detect the

low-level jet we have suggested a procedure that relates the 500-m profiler wind speeds to the tower wind speeds extrapolated upward to 500 m. This method will utilize the expected error in extrapolation to determine if the low-level jet is present and, if present, its general location. It is believed that the outlying points produced from plotting the profiler winds against the extrapolated winds will be key in determining the location of the low-level jet. Figure 4.14 provides the wind profile that would be expected if there is a good correlation between the 500-m profiler wind speed and the wind speed extrapolated to 500 m from the tower data. A good correlation would also be present to obtain a wind profile like the one shown in Figure 4.15. In Figure 4.15 the low-level jet is located above 500 m so it would not be detectable when observing the 500-m winds. Figure 4.16 shows the expected wind profile of the outliers at lower wind speeds. In this case the extrapolated 500-m wind speed is underestimated because the low-level jet is above 100 m, but the 500-m height is within the low-level jet. Figure 4.17 provides the expected wind profile in the case that the low-level jet is below 500 m and occurring at the 100-m height. In this case the extrapolated winds will overestimate the 500-m wind speed and more outliers will be present in the higher wind speed area.

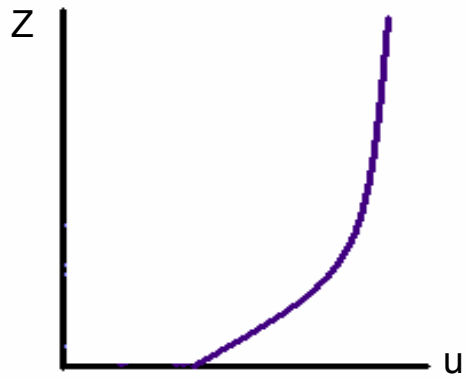


Figure 4.14. Wind profile for a case where a low-level jet is not present.

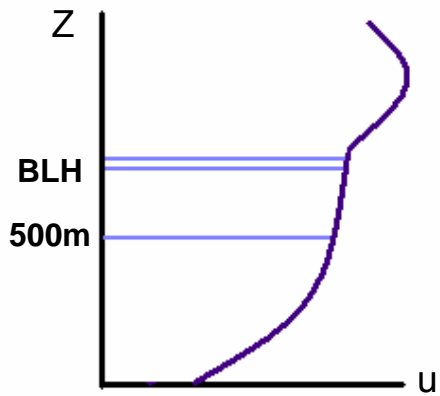


Figure 4.15. The wind profile when the low-level jet is above 500 m. BLH is the height of the boundary layer.

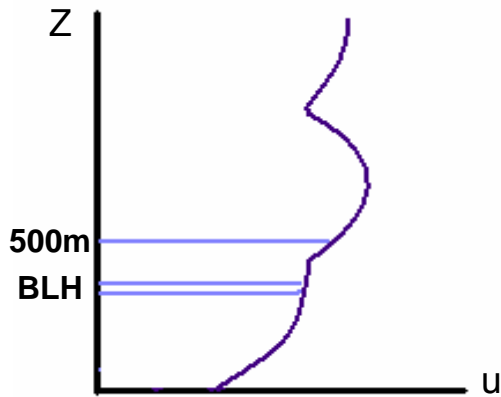


Figure 4.16. The low-level jet is located completely above the 100-m tower height, but intersects the 500-m level. BLH is the height of the boundary layer.

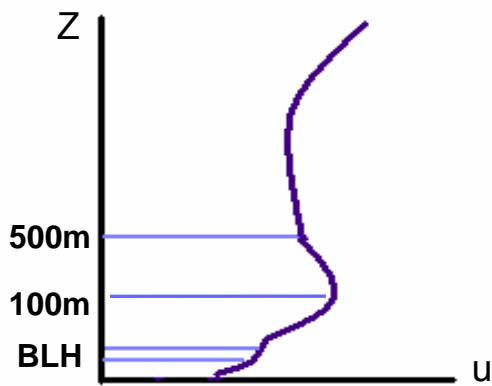


Figure 4.17. The low-level jet is located completely below the 500-m height, but is present at the 100-m level. BLH is the height of the boundary layer.

To determine which wind profile is dominant in a month of tower data we had to create plots of the profiler wind speed at 500 m versus the tower data extrapolated to 500 m using the logarithmic wind profile law given by the following equation taken from Arya (1998).

$$\frac{U}{u_*} = \frac{1}{\kappa} \ln\left(\frac{z}{z_0}\right) \quad (4.2)$$

Then using the theory stated above we would be able to classify the scatter plot produced based on the location of the majority of outliers. In creating the plots all data with a wind speed less than 3 m/s was excluded. Figures 4.18 through 4.20 provide examples of each case. Figure 4.18 represents a good correlation since the majority of points are found within the standard deviation range. So, a wind profile such as that found in Figure 4.14 and 4.15 would be expected for the points within the standard deviation range. More outliers are found below the negative standard deviation line for Figure 4.19 meaning that the extrapolated wind speed has been underestimated and a high LLJ is detected because the jet is located near 500 m. Thus, Figure 4.16 would be the wind profile matching the outliers located below the negative standard deviation line. In Figure 4.20 there are more incidences of the low-level jet being located at 100 m and completely below 500 m because more outliers are found above the positive standard deviation line. These outliers should correspond to the wind profile provided in Figure 4.17 and would be considered a low LLJ occurrence. Thus, this method makes it very easy to determine the presence of the LLJ and its general location by looking at each outlier. Table 4.8 was then produced to provide the number of outliers above and below the standard deviation lines to further assess the number of LLJ cases occurring within a month. Since it is difficult to determine the dominant location of the LLJ for a month of data by looking at the scatter plots, Table 4.8 is very valuable. Using this table it is easier to detect which case is dominant for each month by noting the number of occurrences. Table 4.8 also

lists the standard deviation used for each month and the correlation coefficient obtained for the relationship between the extrapolated wind speed and the profiler wind speed.

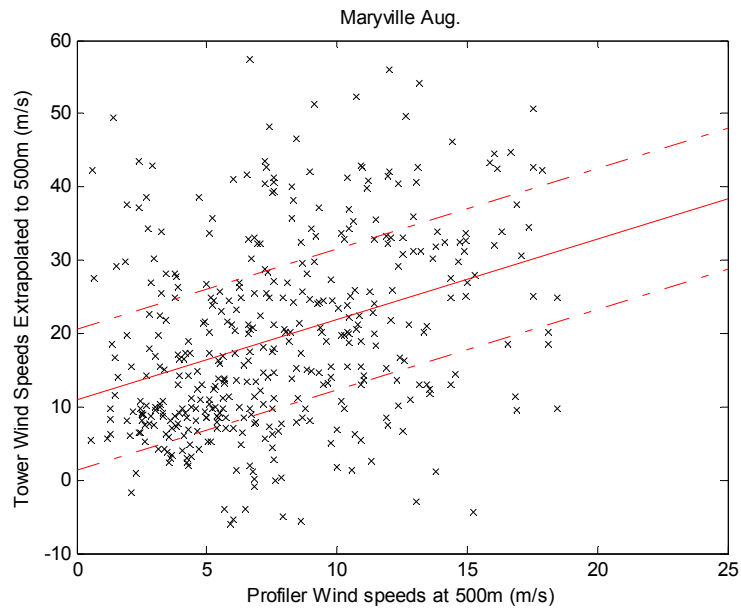


Figure 4.18. Extrapolated tower winds to 500 m versus profiler winds at 500 m. The solid red line is the average and the dashed red lines are the average plus or minus the standard deviation. This case shows an occurrence of good correlation since most of the data points are within the standard deviation range.

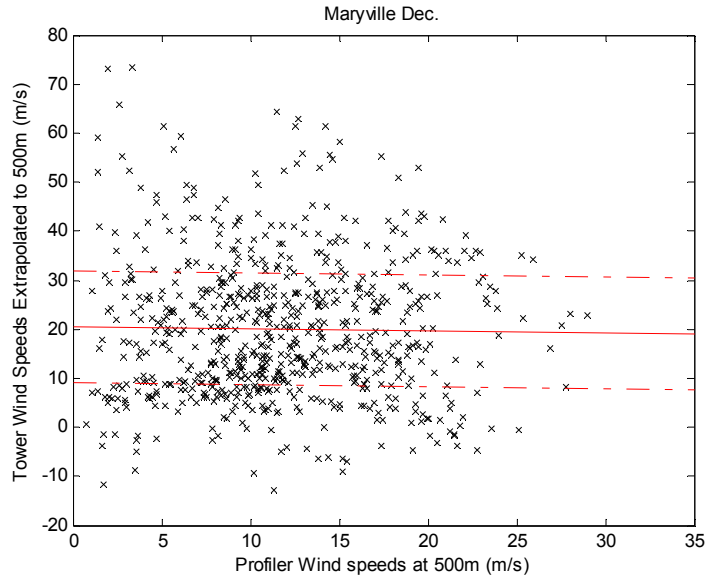


Figure 4.19. Extrapolated tower winds to 500 m versus profiler winds at 500 m. The solid red line is the average and the dashed red lines are the average plus or minus the standard deviation. This case has more incidences of the LLJ being present higher up, nearer to 500 m, because the number of outliers below the standard deviation line exceeds the number above.

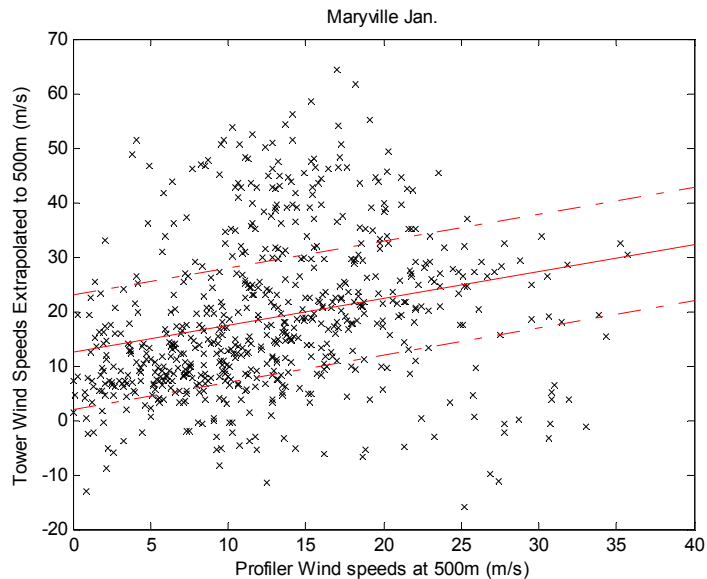


Figure 4.20. Extrapolated tower winds to 500 m versus profiler winds at 500 m. The solid red line is the average and the dashed red lines are the average plus or minus the standard deviation. This case shows a higher incidence of a LLJ being present at 100 m and completely below 500 m since the number of outliers above the standard deviation line exceeds the number below.

Tower	Month	Correlation	Standard Deviation	# of high LLJ outliers	# of low LLJ outliers
Blanchard	August	0.487	8.63	81	86
	September	0.534	7.99	102	99
	October	0.450	8.16	94	97
	November	0.316	9.09	94	86
	December	0.273	9.24	168	149
	January	0.554	8.12	61	71
	February	0.382	8.05	130	117
	March	0.429	6.45	149	126
	Chillicothe	October	0.242	7.58	86
November		0.074	7.73	100	96
December		0.181	6.60	129	137
January		0.364	6.60	133	134
February		0.265	7.55	153	125
March		0.246	7.94	166	144
Maryville	August	0.351	9.64	79	80
	September	0.424	8.87	89	99
	October	0.013	11.60	113	102
	November	0.150	11.20	89	90
	December	-0.017	11.42	156	137
	January	0.250	10.51	119	128
	February	0.272	9.80	118	113
	March	0.081	10.54	143	148
Miami	July	0.544	9.28	92	104
	August	0.683	7.58	92	96
	September	0.415	10.59	78	82
	October	0.539	9.58	96	96
	November	0.464	10.37	84	92
	December	0.222	10.15	138	123
	January	0.398	9.09	115	112
	February	0.377	8.97	121	128
	March	0.368	9.80	166	145
	Raytown	August	0.540	8.35	83
September		0.511	8.76	81	68
October		0.464	8.98	101	84
November		0.380	10.44	82	77
December		0.289	10.29	125	128
January		0.387	9.87	130	109
February		0.469	8.83	120	107
March		0.321	8.96	151	133

Table 4.8. The correlation coefficient for the relationship between the extrapolated tower wind to 500 m and the profiler wind speed at 500 m. Also given is the standard deviation used to locate the number of outliers and the

number of outliers present indicating a high LLJ occurrence (the LLJ is near 500 m) or a low LLJ occurrence (the LLJ is near 100 m).

To better relate the number of high and low LLJ points a chart was prepared to determine the percent of time the high or low LLJ was present. These charts are provided in Figures 4.21 and 4.22. These charts were made because there are different amounts of data available for each tower at each month. In the event of icing, one tower may thaw out sooner than another and begin to record measurements at an earlier time. This would allow a greater number of observations for one site and possibly a greater number of LLJ occurrences as well. To account for differences in the number of data points the number of low and high LLJ occurrences was divided by the total number of observational measurements for each month for each tower. The results are given in Figures 4.21 and 4.22 for the low and high LLJ occurrences respectively. These figures show that the proportionality of the LLJ occurrences is fairly steady and only varies by a few percentage points. This signifies that the LLJ possibly occurs on a regular basis or at least often enough to impact wind speeds.

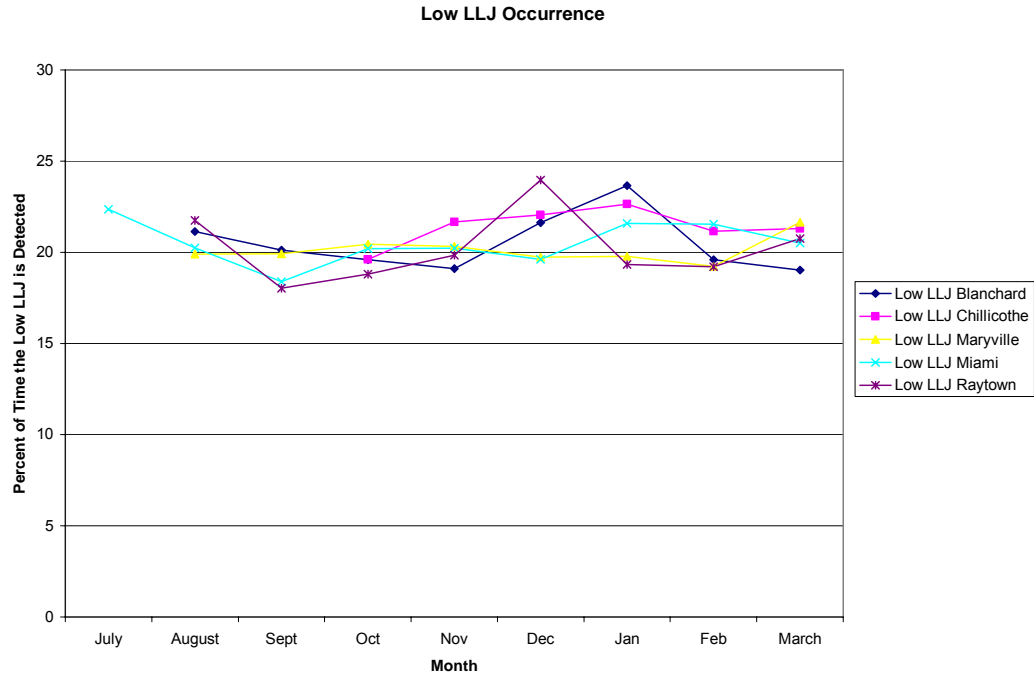


Figure 4.21. The percentage of low LLJ occurrences for each month is presented. The percentage was obtained by dividing the number of low LLJ occurrences by the number of data points for each month.

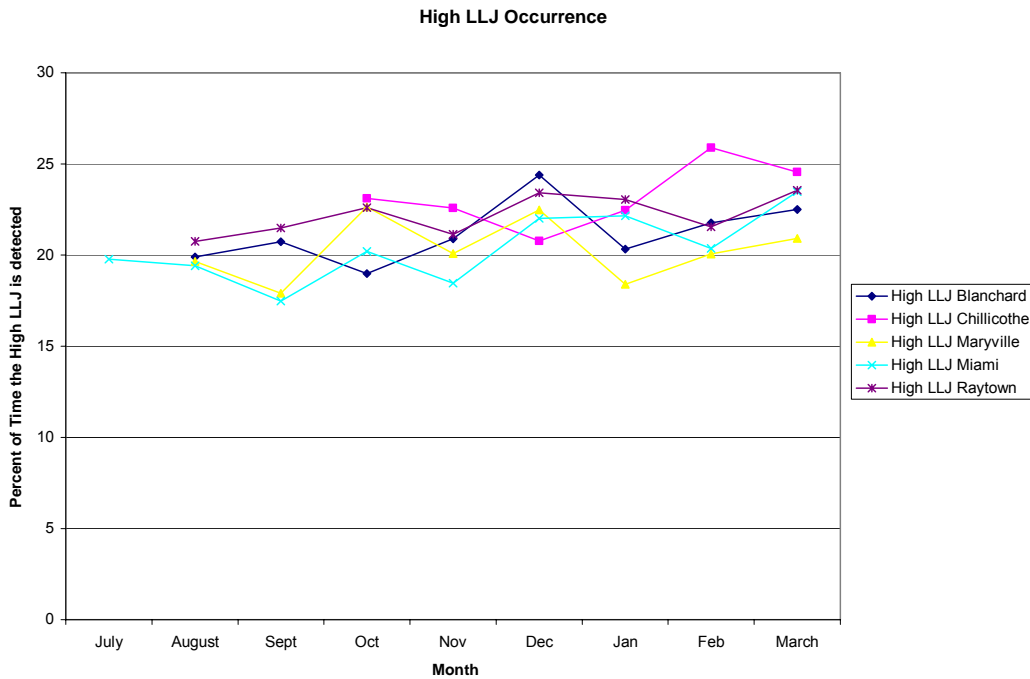


Figure 4.22. The percentage of high LLJ occurrences for each month is presented. The percentage was obtained by dividing the number of high LLJ occurrences by the number of data points for each month.

Now that occurrences of the LLJ have been identified we must test to see if the outlying points found are actually detecting a LLJ phenomenon. To look into this we must first determine the time of each outlying occurrence. The times of the occurrences are given in Figures 4.23 through 4.28. The months of September, December, and March were chosen because they were evenly spaced among the period of record for the dataset. The wind speeds from the observational data are given at each time to observe the strength of the wind associated with the supposed jet for the point in question. The cases have been separated between high and low LLJ occurrences. When looking at the entire month of data for Figures 4.23 through 4.28 it is difficult to pick out any particular pattern among the tower data. A pattern would indicate that the outliers located are not just an abnormality, but are occurring at each site at the same times and may show the presence of the LLJ. Since the pattern was difficult to distinguish among the entire month of data it was sectioned out into five day periods so the occurrences could be viewed more clearly. For this reason one of the neater five day periods is provided for each month.

The pattern we are looking for is best shown in Figure 4.28 for the month of March. During days ten through fifteen three good correlations can be found. The Blanchard data was not working properly at this time for the month of March and that is the reason it is not present, but the other four towers are in good agreement. The three periods of good agreement fall between days 10.7 and 11.2, 11.5 and 12.1, and 12.5 and 13. We would expect to find a LLJ occurrence

for these time periods. There are also extra times where just one or two towers will depict the presence of a LLJ through a blip on the chart. An example of this occurs in Figure 4.28 between the days 14.5 and 15. It may be that the LLJ is just limited in area, but for the most part these are not believed to be LLJ cases and would need further examination for this to be proven. Even the cases we believe to be representative of a LLJ would need further verification to prove that this method for detecting the LLJ is working properly. This is a task to be handled in future research by comparing the times at which the outlying points occur to times where the LLJ is known to be present from other sources such as reanalysis fields.

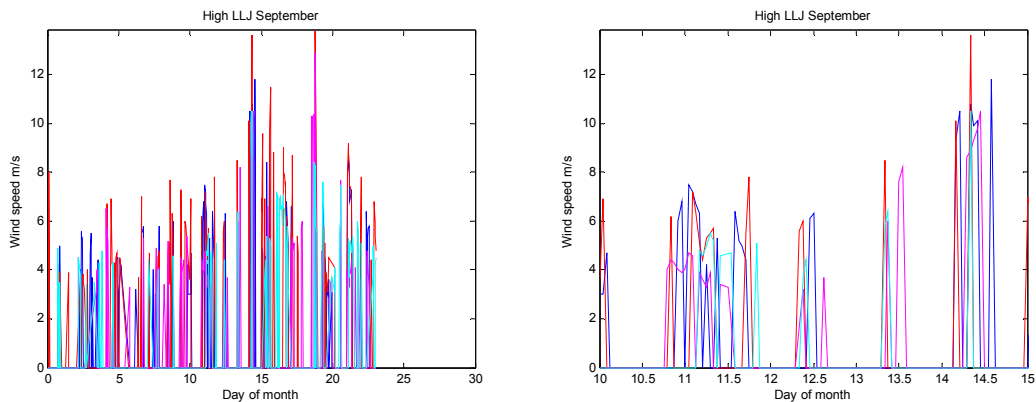


Figure 4.23. Displayed are the times the high LLJ is detected and the wind speed present at the time of detection for the month of September. The blue line represents the data from the Maryville tower, the red line is for the Blanchard tower data, the magenta line is the Miami data and the cyan line is the Raytown data.

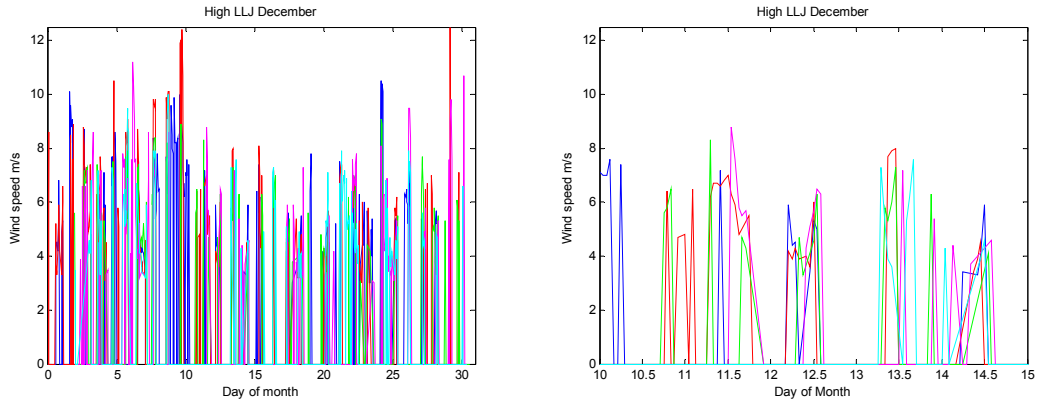


Figure 4.24. Displayed are the times the high LLJ is detected and the wind speed present at the time of detection for the month of December. The blue line represents the data from the Maryville tower, the red line is for the Blanchard tower data, the green line is the Chillicothe data, the magenta line is the Miami data and the cyan line is the Raytown data.

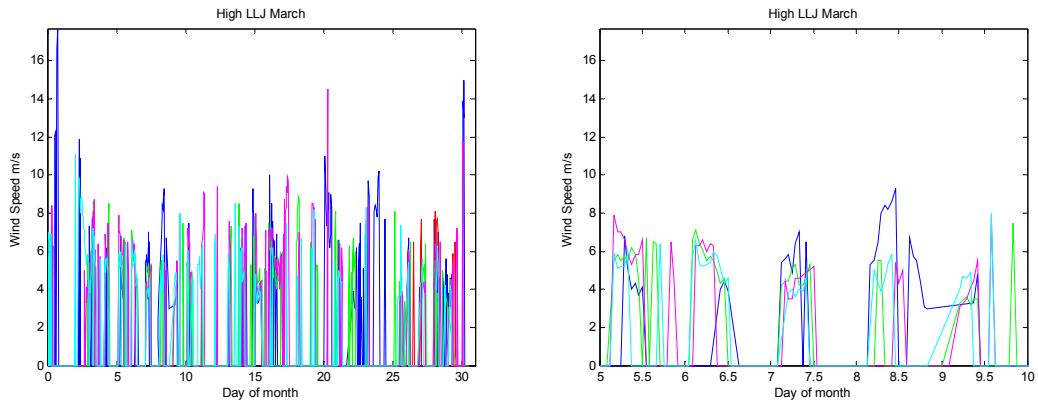


Figure 4.25. Displayed are the times the high LLJ is detected and the wind speed present at the time of detection for the month of March. The blue line represents the data from the Maryville tower, the red line is for the Blanchard tower data, the green line is the Chillicothe data, the magenta line is the Miami data and the cyan line is the Raytown data.

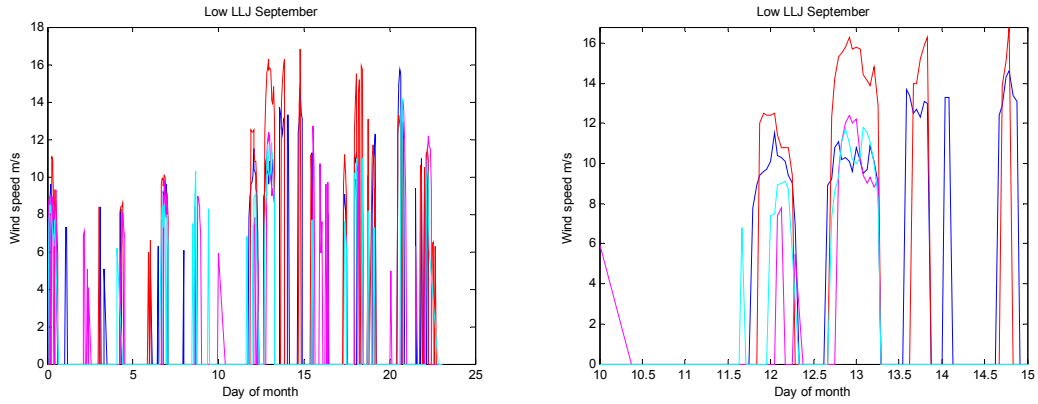


Figure 4.26. Displayed are the times the low LLJ is detected and the wind speed present at the time of detection for the month of September. The blue line represents the data from the Maryville tower, the red line is for the Blanchard tower data, the magenta line is the Miami data and the cyan line is the Raytown data.

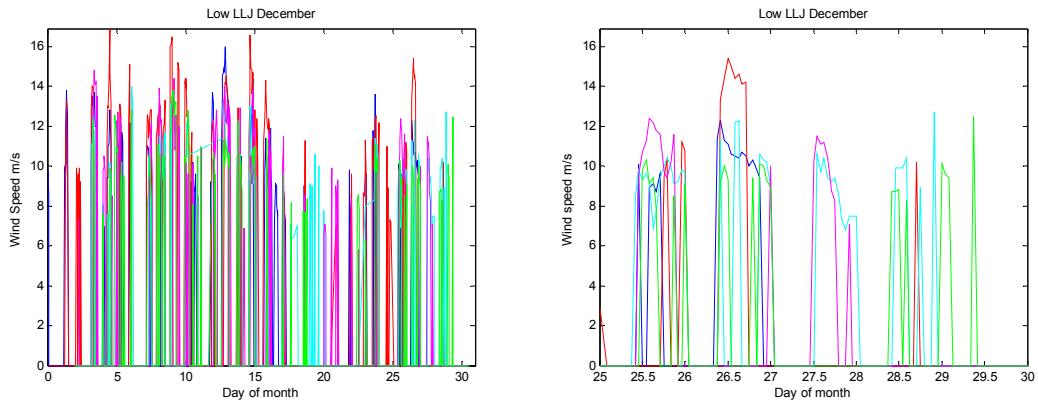


Figure 4.27. Displayed are the times the low LLJ is detected and the wind speed present at the time of detection for the month of December. The blue line represents the data from the Maryville tower, the red line is for the Blanchard tower data, the green line is the Chillicothe data, the magenta line is the Miami data and the cyan line is the Raytown data.

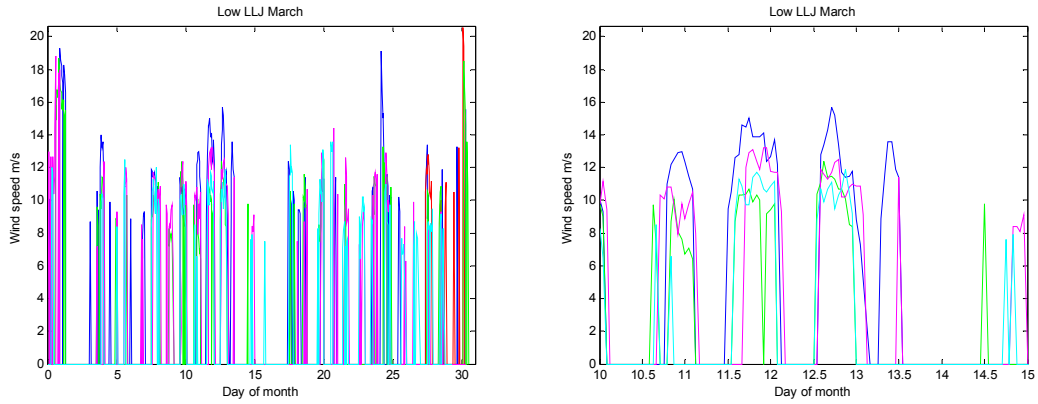


Figure 4.28. Displayed are the times the low LLJ is detected and the wind speed present at the time of detection for the month of March. The blue line represents the data from the Maryville tower, the red line is for the Blanchard tower data, the green line is the Chillicothe data, the magenta line is the Miami data and the cyan line is the Raytown data.

Chapter 5 Conclusions and Future Directions

5.1 Conclusions

This study has provided a great amount of data to further wind resource estimates and research in the state of Missouri. A tall tower network has been established in Northwest Missouri that will aid in the development of wind energy resources. During the period of this project, some eager developers even placed wind turbines in areas of Northwestern Missouri and are currently generating electricity through these turbines. The generation of wind energy in the state of Missouri is a very exciting and liberating advancement, and the goals of this project provide a solid foundation for siting areas for development and learning more about the available resources.

5.1.1 Verification of Current Wind Maps

The Arc GIS wind map created by AWS Truewind Ltd.- commissioned by Missouri DNR- provides a good representation of the available wind energy resources for the state of Missouri. This was shown through our rough verification of the wind map using the observational data taken from the tower sites. This finding is important because we can now trust that the wind map is fairly accurate in locating areas where strong wind speeds are present.

Quantifying how correct the wind speed estimates are is a project that could be performed in the future, once more data has been collected. Further investigation in this area may better explain why the observational data was found to present weaker wind speeds than the wind maps.

5.1.2 Diurnal Variation

The diurnal variation plots produced using the observational tower data matched well with the expected pattern. Of interest was the rise in wind speeds in the winter and early spring months. It appears that the best wind energy production would occur during this period as well. These seasonal variations in wind speed may also be attributed to the strengthening of the nocturnal low-level jet during the winter months. The diurnal variation pattern does provide a good validation of the observed data and this will allow for further applications to be performed using the dataset.

5.1.3 The Use of Profiler Winds as a Proxy for Surface Winds

Profiler winds do not appear to be a good estimate for surface winds when extrapolated downward. This can be attributed to the influence of roughness features on surface winds that is not present at the 500-m level. The boundary layer is also believed to play a role in the correlation between the profiler winds to the extrapolated surface winds. More work may help this area since the dataset

is so large, and the correlation coefficients may be more important than they appear at first glance. It was also found that when pairing profiler winds with observed winds the direction of the tower from the profiler may influence the correlation between the two. Nevertheless, it has been decided that extrapolating surface winds upward, as is the normal procedure, tends to work better than extrapolating 500-m winds downward.

5.1.4 Locating the Low Level Jet

Locating the low-level jet using the known error in extrapolating surface winds to 500 m should provide a good method of detection for the low-level jet. Although, more work is necessary to determine if the outliers found are actually representative of LLJ cases, this is a promising detection method as has been shown by the research conducted in this study. The reasoning seems sound, and thus far seems to be a fairly good method of determining the presence of a LLJ and whether it is located higher or lower in the atmosphere.

5.2 Future Directions

Once the observational data has been collected for a period of one year, it will prove to be much more useful. With a year of data all seasonal variations will be accounted for and the wind maps could be verified in a quantitative manner. It would also be possible to determine if Missouri is a good area for wind energy

development. More studies could be performed on the low-level jet and detection of this phenomenon. The method employed in this study to determine the location of the LLJ will also need further examination and the points indicating high and low LLJs will need to be verified in future research to validate the method described earlier. There is also a large amount of data available that was not utilized in this project such as wind shears and histograms. The wind direction was overlooked as well. Therefore, future projects could examine wind shear characteristics, wind roses could be observed and directional significance accounted for. It would also be of great importance to further discover the relationship between remote sensing networks and observational networks so a complete wind profile could be obtained for the atmosphere. This would provide many benefits to wind energy development as well as wind analysis.

References

- AMS, 2007: Glossary of Meteorology.
<http://amsglossary.allenpress.com/glossary>. accessed (24 Jan. 2007).
- Arya, S. Pal, 1998. Introduction to Micrometeorology. San Diego, CA: Academic Press, 420.
- AWEA, 2003: How Wind Works. American Wind Energy Association.
<http://www.awea.org/pubs/factsheets/HowWindWorks2003.pdf> accessed (23 Apr. 2007).
- Banta, R. M., Kelley, N. D. and Pichugina, Y. L, 2004: Low-Level Jet Properties and Turbulence below the Jet during the Lamar Low-Level Jet Project. Preprints, 16th Symp. On Boundary Layers and Turbulence, Portland, ME, American Meteorological Society, CD-ROM, 4.10.
- Banta, R.M., Pichugina, Y.L. and Brewer, W.A., 2006: Turbulent Velocity-Variance Profiles in the Stable Boundary Layer Generated by a Nocturnal Low-Level Jet. *Journal of the Atmospheric Sciences*, **63**, 2700-2719.
- Blackadar, A.K., 1957: Boundary Layer Wind Maxima and their Significance for the Growth of Nocturnal Inversions. *Bulletin of the American Meteorological Society*, **38**, 283-290.
- Blackler, T. and Iqbal, M., 2005: Pre-feasibility Study of Wind Power Generation In Holyrood, Newfoundland. *Renewable Energy*, **31**, 489-502.
- Bossanyi, E., Burton, T., Sharpe, D. and Jenkins, N, 2001: Wind Energy Handbook. West Sussex, England: John Wiley & Sons Ltd, 617.
- Brower, M., 2005. AWS Truewind- Wind Energy Resource Maps of Missouri. Available from Missouri Department of Natural Resources, CD-ROM.
- BWEA, 2006: Wind Energy Technology. British Wind Energy Association.
<http://www.bwea.com/ref/tech.html>. accessed (5 Apr. 2007).
- Carlin, P., 2004: A suggested Modification to a Common Expression for the Energy Content of a Wind Data Sample. *Wind Energy*, **8**, 477-480.
- Dabberdt, W., 1968: Tower-Induced Errors in Wind Profile Measurements. *Journal of Applied Meteorology*, **7**, 359-366.

- Danish Wind Industry Association, 2003: Wind & Turbine Siting, www.windpower.org. accessed (23 Apr. 2007).
- Djuric, D., 1994. Weather Analysis. Prentice Hall, Upper Saddle River, NJ, 304.
- Houghton, J.T., Ding, Y., Griggs, D.J., Noguer, M., van der Linden, P.J., Dai, X., Maskell, K. and Johnson, C.A. (eds.), 2001: IPCC, 2001: Climate Change 2001: The Scientific Basis. Contribution of Working Group I to the Third Assessment Report of the Intergovernmental Panel on Climate Change, 881.
- Kelley, N., Shirazi, M., Jager, D., Wilde, S., Adams, J., Buhl, M., Sullivan, P. and Patton, E., 2004: Lamar Low-Level Jet Project Interim Report. National Renewable Energy Laboratory and the National Center for Atmospheric Research. Available on-line at http://www.osti.gov/bridge/product.biblio.jsp?osti_id=15006544.
- Kobayashi, T., Adachi, A., Gage, K.S., Carter, D.A., Hartten, L.M., Clark, W.L., and Fukuda, M., 2005: Evaluation of Three-Beam and Four-Beam Profiler Wind Measurement Techniques Using a Five-Beam Wind Profiler and Collocated Meteorological Tower. *Journal of Atmospheric and Oceanic Technology*, **22**, 1167-1180.
- Landberg, L., Myllerup, L., Rathmann, O., Petersen, E., Jorgensen, B., Badger, J. and Mortensen, N., 2003: Wind Resource Estimation-An Overview. *Wind Energy*, **6**, 261-271.
- Lock, A.P., 2000: The Numerical Representation of Entrainment in Parameterizations of Boundary Layer Turbulent Mixing. *Monthly Weather Review*, **129**, 1148-1163.
- Lundquist, J.K., 2005: Interaction of Nocturnal Low-Level Jets with Urban Geometries as seen in Joint URBAN 2003 Data. Preprints, 6th Symp. On the Urban Environment, Atlanta, GA, American Meteorological Society, available on-line at <http://www.llnl.gov/tid/lof/documents/pdf/322307.pdf>.
- Lupo, A.R., Kelsey, E.P., Weitlich D.K., Mokhov I.I., Akyuz F.A., Guinan, P.E., Woolard J.E., 2007: Interannual and Interdecadal Variability in the Predominant Pacific Region SST Anomaly Patterns and their impact on a Local Climate. *Atmosfera*, **20**, 171- 196.
- NOAA, 2005. Global Systems Division NOAA Profiler Network, <http://www.profiler.noaa.gov/npn/aboutProfilerData.jsp> accessed (30 Mar. 2006).

- OFCM, 2006: U.S. Wind Profilers. Office of the Federal Coordinator of Meteorology. <http://www.ofcm.gov/r14/contents.htm> accessed (30 Mar. 2006).
- Petersen, E., Mortensen, N., Landberg, L., Hojstrup, J. and Frank, H., 1998a: Wind Power Meteorology. Part I: Climate and Turbulence. *Wind Energy*, **1**, 25-45.
- Petersen, E., Mortensen, N., Landberg, L., Hojstrup, J. and Frank, H., 1998b: Wind Power Meteorology. Part II: Siting and Models. *Wind Energy*, **1**, 55-72.
- Pichugina, Y.L., Banta, R.M., Kelley, N.D., Sandberg, S.P., Machol, J.L. and Brewer, W.A., 2004: Nocturnal Low-Level Jet Characteristics Over Southern Colorado. Preprints, 16th Symp. On Boundary Layers and Turbulence, Portland, ME, American Meteorological Society, CD-ROM, 4.11.
- Pitchford, K.L. and London, J., 1961: The Low-Level Jet as Related to Nocturnal Thunderstorms over Midwest United States. *Journal of Applied Meteorology*, **1**, 43-47.
- Portman, D., 2004: The Nocturnal Low-Level Jet. <http://www.windwisdom.net/nllj.htm>. accessed (22 Apr. 2007).
- Schwartz, M., Elliot, D., 2005: Towards a Wind Energy Climatology at Advanced Turbine Hub-Heights. Preprint, 15th Conference on Applied Climatology, Savannah, GA, American Meteorological Society.
- Schwartz, M., Elliot, D., 2006: Wind Shear Characteristics at Central Plains Tall Towers. Preprint, Wind Power 2006 Conference, Pittsburgh, PA, American Wind Energy Association.
- US EPA. 21 Dec. 2006. U.S. Environmental Protection Agency, <http://epa.gov/climatechange/science/recentac.html> (5 Feb. 2007).
- Wind Speed of Missouri at 100 Meters. AWS Truewind, http://www.awstruewind.com/inner/windmaps/maps/NorthAmerica/UnitedStates/Missouri/MO_SPD100m.pdf (15 Feb. 2007).